nature medicine

Article

https://doi.org/10.1038/s41591-024-03277-z

Sustained HIV remission after allogeneic hematopoietic stem cell transplantation with wild-type CCR5 donor cells

Received: 6 June 2024

Accepted: 27 August 2024

Published online: 2 September 2024

Check for updates

A list of authors and their affiliations appears at the end of the paper

HIV cure has been reported for five individuals who underwent allogeneic hematopoietic stem cell transplantation (allo-HSCT) with cells from *CCR5Δ32* homozygous donors. By contrast, viral rebound has occurred in other people living with HIV who interrupted antiretroviral treatment after undergoing allo-HSCT, with cells mostly from wild-type *CCR5* donors. Here we report the case of a male individual who has achieved durable HIV remission following allo-HSCT with cells from an unrelated HLA-matched (9 of 10 matching for *HLA-A*, *HLA-B*, *HLA-C*, *HLA-DRB1* and *HLA-DQB1* alleles) wild-type *CCR5* donor to treat an extramedullary myeloid tumor. To date, plasma viral load has remained undetectable for 32 months after the interruption of antiretroviral treatment. Treatment with ruxolitinib has been maintained during this period to treat chronic graft-versus-host disease. Low levels of proviral DNA were detected sporadically after allo-HSCT, including defective but not intact HIV DNA. No virus could be amplified in cultures of $CD4^+$ T cells obtained after antiretroviral treatment interruption, while $CD4^+$ T cells remained susceptible to HIV-1 infection in vitro. Declines in HIV antibodies and undetectable HIV-specific T cell responses further corroborate the absence of viral rebound after antiretroviral treatment interruption. These results suggest that HIV remission could be achieved in the context of allo-HSCT with wild-type *CCR5*.

Antiretroviral treatment (ART) efficiently blocks viral replication of HIV but cannot eliminate infected cells, which persist in people with HIV despite decades of treatment. These persistently infected cells establish viral reservoirs that initiate rapid viral rebound if ART is interrupted. A few exceptions have been reported for individuals who are able to durably control HIV-1 infection after discontinuation of ART, achieving a state of virological remission[1,2]. This outcome appears to be favored by early ART initiation[3,4], although the mechanisms remain unknown. Notably, five individuals have seemingly achieved an HIV cure after undergoing allogeneic hematopoietic stem cell transplantation (allo-HSCT), for the treatment of different blood cancers, with cells from *CCR5Δ32/Δ32* donors[5–9]. These donors' cells lack CCR5 expression on the cell surface, thus providing natural protection against CCR5-tropic HIV-1 variants[10].

Different studies have shown that allo-HSCT in people with HIV consistently provokes a dramatic decrease in the frequency of HIV-infected cells[11–14]. The reduction in the size of the HIV reservoir is unrelated to the presence (or absence) of the *CCR5Δ32* mutation in donor cells[15]. Instead, it seems to result from a combination of cytotoxic effects of the conditioning regimens, donor allogeneic immunity during graft-versus-host reactions and the gradual dilution of the pool of infected cells during immune cell replacement[12,16]. However, even such pressure may not be sufficient to eliminate all infected cells. Cells carrying HIV DNA have been found after allo-HSCT in the blood of some

e-mail: asier.saez-cirion@pasteur.fr; alexandra.calmy@hug.ch

people with HIV who did not achieve full donor chimerism[12,17] or in tissue sanctuaries analyzed in necropsy studies[18]. Moreover, during the weeks following allo-HSCT, a window of vulnerability occurs when highly activated CD4$^+$ T cells from both donor and recipient coexist[19], thereby increasing the risk of reservoir reseeding if infection of donor cells is not prevented by pharmacological or genetic and host barriers. Accordingly, and in contrast to the five individuals who have achieved HIV cure, viral rebound has been reported so far in all cases of people with HIV who interrupted ART after receiving allo-HSCT from wild-type *CCR5* donors[11–15], and even in some individuals who received a transplant from *CCR5Δ32/Δ32* donors[20]. These observations strongly supported the hypothesis that engraftment with CD4$^+$ T cells that remain resistant to preexisting HIV-1 variants might be necessary to avoid HIV-1 relapse from the few infected cells that may persist after allo-HSCT.

Challenging this assumption, we describe here the case of a male individual living with HIV-1 for over 30 years who, 72 months after undergoing allo-HSCT with cells from a wild-type *CCR5* donor and 32 months after ART interruption, has not shown evidence of HIV-1 rebound or replicating virus despite carrying CD4$^+$ T cells that remain fully susceptible to HIV-1 infection.

Results

Case study

We conducted a longitudinal virological and immunological characterization of a 53-year-old male (IciStem number 34, IciS-34), who is alive and asymptomatic. This individual was diagnosed to be HIV-1 clade B positive in May 1990 in Switzerland and presented with a CD4$^+$ T cell count of 589 cells per microliter (32%) at the time of diagnosis (category A1 according to US Centers for Disease Control and Prevention classification). He immediately started ART after diagnosis, including first-generation nucleoside reverse transcriptase inhibitors (Supplementary Fig. 1). However, despite antiretroviral exposure, his CD4$^+$ T cell count decreased to 295 cells per microliter and the first available HIV-1 plasma viral load determination in October 1996 was 63,293 copies per milliliter (Fig. 1). At this time, he began protease inhibitor-based therapy, receiving sequentially boosted saquinavir and atazanavir, without achieving full viral suppression (median (interquartile range), 1,150 (102–7,745) HIV RNA copies per milliliter) during this period that lasted 9 years. A lopinavir-based therapy was initiated in October 2005, resulting in a continuously suppressed plasma viral load despite evidence of multiresistance to components of three major classes of antiretrovirals (Supplementary Table 1). A progressive increase in CD4$^+$ T cell counts and normalization of the CD4/CD8 ratio were also observed (Fig. 1). An integrase-inhibitor-based ART regimen with dolutegravir and darunavir/ritonavir (DRV/r) was initiated in January 2015. This individual has been followed in the Swiss HIV cohort study since April 1992.

In January 2018, this person was diagnosed with a myeloid sarcoma with lymph node and bone marrow involvement. He initially received two cycles of induction chemotherapy based on anthracyclines, fludarabine and cytarabine. To avoid drug–drug interactions, DRV/r was switched to tenofovir alafenamide and emtricitabine (200/25 mg) in March 2018 (Fig. 1 and Supplementary Fig. 1). He experienced a short-term malignancy relapse in June 2018 and was treated with a hypomethylating agent, followed by allo-HSCT in July 2018. The donor was an unrelated nine-of-ten HLA-matched (Supplementary Table 2) male with no *CCR5Δ32* mutation. IciS-34 received one cycle of a sequential conditioning regimen (clofarabine, cyclophosphamide, fludarabine and a total body irradiation of 8 Gy) before the peripheral stem cell (no T cell depletion) transplant. Graft-versus-host disease (GvHD) prophylaxis after transplant comprised cyclophosphamide at days 3 and 4, tacrolimus and mycophenolate mofetil. Full donor chimerism in granulocytes and mononuclear cells was achieved in blood and bone marrow less than a month after the transplant. The myeloid sarcoma remains in complete remission. A maintenance treatment with 5-azacytidine was provided from January 2019 to September 2020 (21 cycles of 5-azacytidine, 32.5 mg m^{-2} per day, days 1–5). Severe lymphopenia was initially detected after allo-HSCT. A rapid expansion of NK cells and CD8$^+$ T cells was then observed, followed by CD4$^+$ T cells and B cells (Fig. 1 and Supplementary Fig. 2a). Immune reconstitution was incomplete with relatively low CD4$^+$ T cell counts and an inverse CD4/CD8 ratio, consistent with what others and we have observed for other people with HIV who underwent allo-HSCT[19,21] (Fig. 1).

The individual developed hepatic acute GvHD 120 days after HSCT and was treated with corticosteroids and tacrolimus. Following immunosuppressive drug tapering in March 2019 (8 months after HSCT, M8), he presented with a hepatic GvHD relapse, which was treated with corticosteroids and cyclosporin. In July 2019 (M12), he further developed a mild chronic skin GvHD, and in August 2019, a third-line treatment with ruxolitinib 10 mg twice daily was initiated (Fig. 1 and Supplementary Fig. 1b). Immunosuppressive drugs were then tapered and stopped in early January 2021 (M30). Unfortunately, he had signs of a second hepatic GvHD relapse in late January 2021 and resumed a combined anti-GvHD treatment course including corticosteroid and ruxolitinib, with both prescriptions continued until October 2022 (M51). In November 2022 (M52), an atypical neurological chronic GvHD with neuropathy and small-fiber damage was diagnosed and ruxolitinib 10 mg twice daily was again prescribed together with low-dose prednisone (10 mg per day).

During the multiple episodes of GvHD, to reduce the risk of potential drug interactions, ART was further simplified to dolutegravir and lamivudine dual therapy in December 2019 (M17) and to single dolutegravir, one 50 mg tablet daily, in August 2020 (M25). Finally, on 17 November 2021 (M40), all antiretrovirals were stopped following a consensual decision between the participant and his physician to evaluate the possibility of HIV remission. At the time of this report, 32 months after interruption of ART (M72), plasma HIV viremia has remained undetectable despite frequent testing (at least monthly since ART interruption) (Fig. 1).

Decline of virologic markers after allo-HSCT

We further examined virological markers to better characterize the evolution of HIV-1 infection following allo-HSCT and ART interruption in this individual. HIV RNA could be detected with the ultrasensitive viral load assay in three plasma samples obtained before (1.33 RNA copies per ml at M3), at the time of (4.18 RNA copies per ml) and immediately after (2.22 RNA copies per ml at M1) allo-HSCT. A positive ultrasensitive viral load value (4 copies per ml) was also detected at M19 after allo-HSCT, but was undetectable (<1 copy per ml) in all the other samples analyzed, including eight samples analyzed after ART interruption (Fig. 2a). Cell-associated HIV DNA could be detected in bone marrow cells, peripheral blood mononuclear cells (PBMCs) and purified blood CD4$^+$ T cells before allo-HSCT (1,096, 202 and 457 copies per million cells, respectively) (Fig. 3b). These frequencies rapidly decreased after allo-HSCT. Viral DNA was still detectable (316 copies) in a bone marrow sample obtained at M1 after allo-HSCT, but was undetectable in subsequent samples (Fig. 2b,c). HIV DNA was sporadically detected in PBMCs with an ultrasensitive assay[22] (maximum of 5 copies per million cells at M47) and purified CD4$^+$ T cells (maximum of 40 copies at M19, coinciding with positive ultrasensitive viral load) but was consecutively undetectable by quantitative PCR in the last 6 samples obtained after ART interruption. HIV DNA was not detected in small biopsies from the small intestine; ascending, transverse, descending and sigmoid colon; cecum; and rectum obtained at M54 (14 months after ART interruption) (<20 copies of HIV DNA per 10^6 cells; 1.4 million cells tested).

We also investigated the presence of replication-competent virus. The intact proviral DNA assay (IPDA)[23] detected potentially intact proviruses in two samples that had been obtained during ART-suppressed viremia 17 and 32 months before allo-HSCT in the context of his participation in the Swiss HIV cohort study (Fig. 2c). By contrast, potentially intact proviruses were never detected following

https://doi.org/10.1038/s41591-024-03277-z

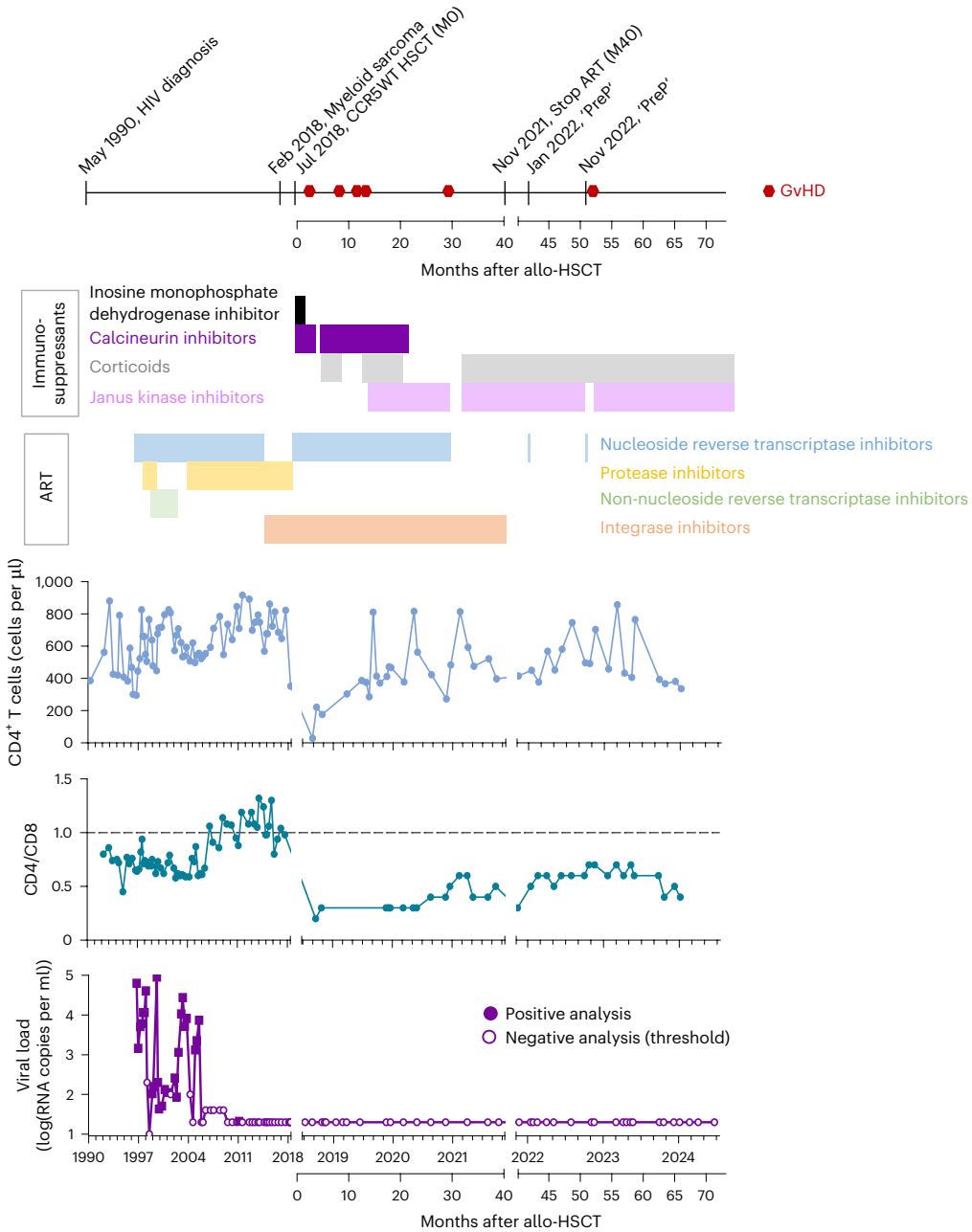

Fig. 1 | Treatment course and immuno-virological evolution. Timeline of clinical events, CD4$^+$ T cell counts, CD4/CD8 ratio and plasma viral load since HIV-1 diagnosis and until last follow-up. The successive immunosuppressants and antiretroviral regimens are also shown (detailed information can be found in Supplementary Fig. 1). Undetectable plasma viral load concentrations are represented by empty symbols at the threshold of detection, which varied throughout the follow-up. Hexagons represent different episodes of GvHD.

allo-HSCT. Traces of defective proviruses were detected in PBMCs and/or bone marrow samples after allo-HSCT by IPDA, at levels over 40 times lower than those observed before allo-HSCT. Intracellular HIV RNA was also not detected in samples obtained at multiple time-points after ART interruption (Supplementary Table 3). Finally, viral production could not be detected with an ultrasensitive p24 single molecule Simoa assay[24] in the supernatants of purified CD4$^+$ T cells from multiple samples that were cultured in the presence of a pool of activated CD4$^+$ T cells from three different donors (Supplementary Table 3). Overall, these results indicate that the HIV-1 reservoir markedly contracted after allo-HSCT in this individual and that, although traces of viral DNA were found in some samples obtained up to 57 months after the transplant, no potentially intact proviruses or evidence of replication-competent viruses were detected after allo-HSCT and ART discontinuation.

Sustained absence of detection of antiretroviral molecules

The participant reported using on-demand pre-exposure prophylaxis during two episodes in January (M42) and November 2022 (M52), taking it for only 2–3 days during these times. To document the ART interruption period more accurately, antiretrovirals were measured retrospectively since November 2022 in all available plasma samples after ART interruption and prospectively from that point onwards. Low concentrations of emtricitabine (2.8–78 ng ml^{-1}) and tenofovir (1–4 ng ml^{-1}) were detected in samples obtained at M42 and M53 (Supplementary Table 4), coinciding with the self-reported use of these molecules by

https://doi.org/10.1038/s41591-024-03277-z

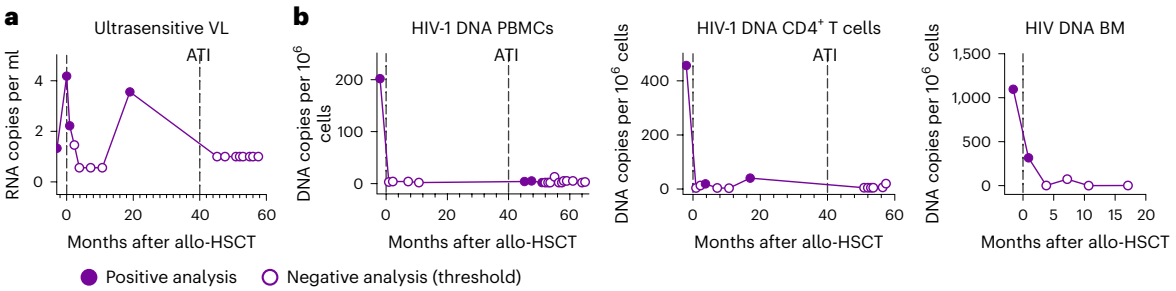

c

	IPDA					
	Blood			Bone marrow		
Months after allo-HSCT	Cells	Intact (copies per 10^6 cells	Defective	Cells	Intact	Defective
−32	681,000	Yes (13)	Yes (137/365,000 droplets)[a]			
−17	965,000	Yes (3)	Yes (80/167,000 droplets)[a]			
0	Allo-HSCT					
1				6,000	No	Yes (2/51,000 droplets)[b]
4	218,000	No	Yes (4/52,000 droplets)[a]	709,000	No	No
19	271,000	No	Yes (9/27,000 droplets)[a]	0.9 million	No	Yes (3/42,000 droplets)[b]
40	ART interruption					
52-1	480,000	No	No			
53	423,000	No	Traces (1/151,000 droplets)[b]			
55	479,000	No	Traces (1/98,000 droplets)[b]			
56	559,000	No	No			
57	360,000	No	Traces (1/75,000 droplets)[b]			
59	695,000	No	No			
61	514,000	No	No			
65	738,000	No	No			

Fig. 2 | Viral markers before and after allo-HSCT. a,**b**, Evolution of residual low-level viremia measured with an ultrasensitive viral load (VL) assay in plasma (**a**) and HIV DNA associated with PBMCs, purified blood CD4$^+$ T cells or bone marrow (BM) cells (**b**) before and after allogeneic HSCT. The empty symbols represent undetectable levels and are shown at the threshold of the techniques, which varied depending on the amount of material analyzed. The time of allo-HSCT and of analytical treatment interruption (ATI) is indicated as a dashed vertical line. **c**, Summary of the outcome of IPDA analyses in blood and tissues at different timepoints before and after allo-HSCT. The number of cells per amount of material tested is indicated for each analysis. [a]Defective in 3′ or 5′. [b]Defective in 3′.

the participant. This is consistent with the concentrations detected being at or below the median plasma concentration levels at 24 h after single oral dose of these molecules reported in the context of the ANRS IPERGAY study[25]. Neither these nor other molecules were found in the other samples analyzed prospectively. These results corroborate that durable remission of HIV infection in this individual occurred in the total absence of antiretroviral molecules for extensive periods of time.

CD4$^+$ T cells remain susceptible to HIV-1 infection

Previous cases of HIV remission following allo-HSCT were associated with the reconstitution of the CD4$^+$ T cell pool with cells that were resistant to R5 HIV-1 due to the *CCR5Δ32* mutation[5–9]. We wondered whether the CD4$^+$ T cells that expanded after allo-HSCT in this individual may possess some alternative mechanism of resistance to HIV-1 infection. As previously reported for other individuals[19], CD4$^+$ T cells from samples obtained early after allo-HSCT were characterized by high activation frequencies (15.5% of HLA-DR$^+$CD38$^+$ cells at M4), which decreased in later samples (2.81% of DR$^+$CD38$^+$ cells at M53) without reaching the basal levels observed in individuals without HIV (Fig. 3a). In agreement with the wild-type *CCR5* status of the donor, CCR5 could be detected on the surface of the CD4$^+$ T cells that expanded after allo-HSCT (Fig. 3b). These cells also expressed CXCR4, which is used by X4 HIV-1 variants. Accordingly, purified CD4$^+$ T cells from IciS-34 obtained after allo-HSCT were highly susceptible to infection in vitro with (R5) HIV-1_{BaL} (Fig. 3c). Moreover, we detected high levels of infected cells after their in vitro exposure to HIV-$1_{NL4\text{-}3}$ΔEnv particles pseudotyped with the pantropic

https://doi.org/10.1038/s41591-024-03277-z

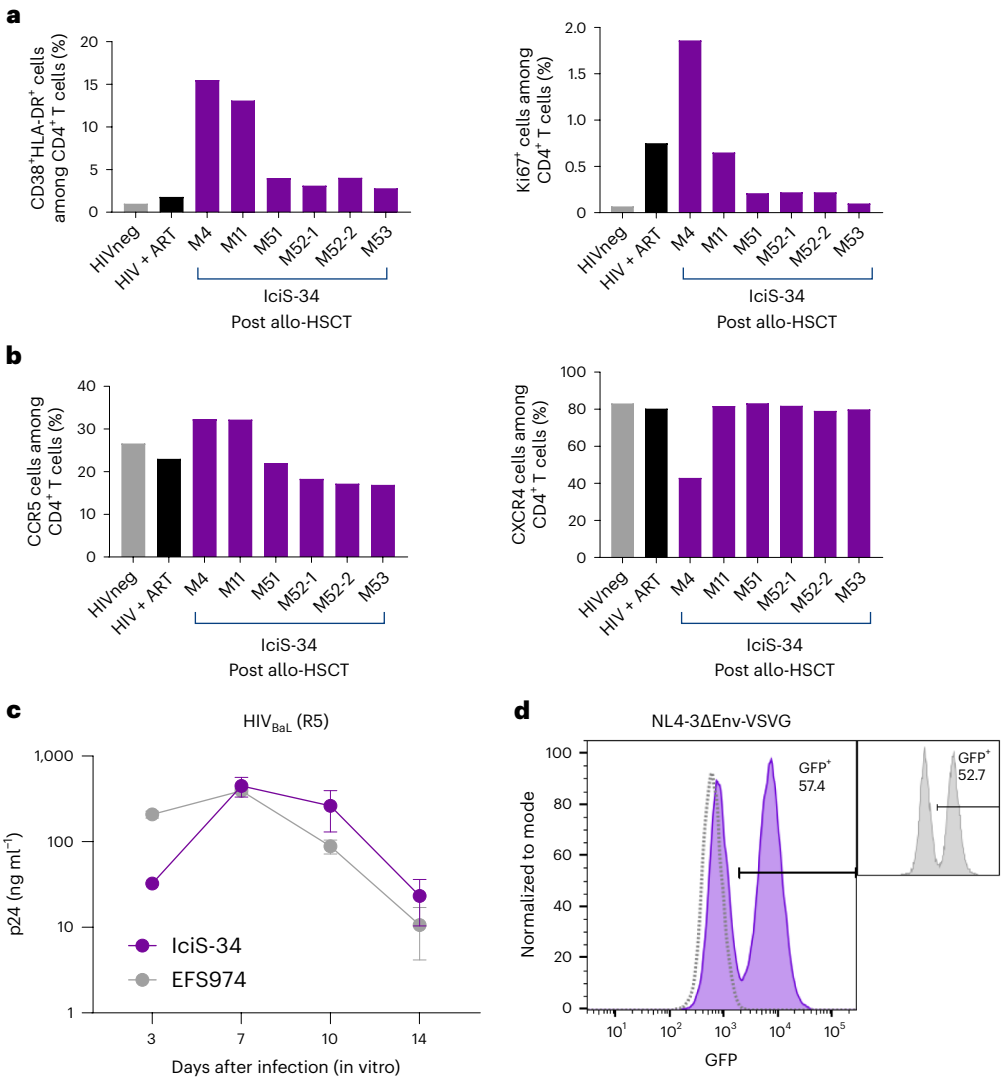

Fig. 3 | Phenotype and HIV susceptibility of CD4⁺ T cells. a,**b**, Percentage of CD4⁺ T cells from IciS-34 expressing activation markers (CD38⁺HLA-DR⁺, Ki67⁺) (**a**) and the HIV-1 coreceptors CCR5 and CXCR4 (**b**) at different times after allo-HSCT (samples designated as the month after allo-HSCT when they were obtained; purple). The proportions of CD4⁺ T cells from an independent HIV-negative (HIVneg) blood donor (gray) and one person with HIV on ART (black) are depicted for reference. **c**, Dynamics of viral replication in purified CD4⁺ T cells from IciS-34 (M59, purple) and one unrelated blood donor upon infection in vitro with HIV-1_{BaL}. The data are shown as the mean ± s.d. ($n = 3$ replicates) of p24 levels in culture supernatants. **d**, Proportion of infected (GFP⁺) CD4⁺ T cells from IciS-34 3 days after challenge with $HIV_{NL4.3GFP}$ΔEnv-VSV-G particles (purple). The negative control is depicted as a dashed line. The rate of infected CD4⁺ T cells from one unrelated blood donor is provided as a reference (gray).

VSV-G envelope (Fig. 3d). These results refuted the presence of intrinsic barriers preventing HIV-1 replication in the CD4⁺ T cells of this individual after transplant.

Waning anti-HIV antibodies

Next, we studied whether the absence of viral rebound could be related to immune control after ART interruption. Immunoblot analyses confirmed the stable presence of anti-HIV antibodies over a period of 20 years preceding allo-HSCT. By contrast, anti-HIV antibodies began to decrease after the intervention, starting with those recognizing p17 and p31, as previously described for other PLWH who underwent allo-HSCT[15] (Fig. 4a). Of note, anti-HIV antibodies continued to wane after ART discontinuation. To characterize the antibody response more thoroughly during this period, we measured the binding of purified IgG antibodies from three plasma samples after ART interruption. IgG antibodies binding to HIV-1 p24, BG505 SOSIP.664 and YU2 gp140 foldon Env trimers, gp120 and gp41 protein subunits were detected in all three samples at low levels, comparable to those found in people who are on ART since primary HIV infection (Fig. 4b). These IgGs showed very weak reactivity against consensus B Env overlapping peptides, including those from gp120 V3 loop and gp41 immunodominant regions commonly detected in other people with HIV (Fig. 4c). Accordingly, purified IgGs showed no neutralizing activity against a panel of five clade B viruses (Fig. 4d), and very weak capacity to bind to CEM.NKR-CCR5 target infected cells (Fig. 4e), and thus may have a limited potential to promote antibody-dependent cellular cytotoxicity. Overall, these results indicate that the absence of viral rebound after ART interruption was not related to an increased pressure by the antibody response.

Absence of detectable HIV-specific T cells

Allo-HSCT was performed with cells from a donor who was matched for HLA-B*27 (Supplementary Table 2), an allele that has previously been shown to favor HIV-1 control[26]. However, we could not detect, by intracellular cytokine staining, CD4⁺ or CD8⁺ T cells responding to 6 h of stimulation with pools of overlapping HIV-1 Gag, Nef or Pol peptides in samples obtained after allo-HSCT (M10) or after ART interruption

(M45 and M64) (Fig. 5a,c). No HIV-specific cells could be amplified either after 6 days of stimulation or recall with HIV-1 peptides (Fig. 5b,c). Moreover, we did not detect $CD8^+$ T cells binding to HLA-B*27 dextramers carrying the immunodominant KRWIILGLNK Gag epitope (Supplementary Fig. 3e). By contrast, cells responding to human cytomegalovirus (HCMV) pp65 peptides could be detected in the same samples and amplified in 6 day cultures (Fig. 5a–c). In agreement with the lack of detection of HIV-specific $CD8^+$ T cells, purified $CD8^+$ T cells obtained at multiple timepoints after ART interruption could not suppress ex vivo HIV-1 infection of autologous $CD4^+$ T cells (Fig. 5d). These results argue against a role of T cells in maintaining viral control in this individual and confirm the overall lack of mobilization of the adaptive response against HIV-1 in this person despite ART discontinuation.

Notably, we observed a relative lack of T cell reactivity in this individual to short polyclonal stimulation when compared with cells from different unrelated blood donors explored in these analyses. We wondered whether this observation could be related to the ruxolitinib-based immunosuppressive therapy[27] that was administered for extended periods of time to treat GvHD. We therefore analyzed the T cell responses in samples taken before, during and after a brief period of ruxolitinib discontinuation that occurred during the follow-up (between M51 and M53; Fig. 5e). Poor polyclonal reactivity was again observed in the M51 sample, when compared with cells from another blood donor (EFS639). The frequency of responding cells sharply increased in the samples taken 2 weeks (M52-1) and 4 weeks (M52-2) after ruxolitinib was stopped. Ruxolitinib was reintroduced at this time owing to relapse of GvHD, and a reduction in the frequency of responding T cells was observed 2 weeks later (M53). These results support that ruxolitinib therapy may influence the reactivity of T cells to short polyclonal stimulation. Of note, despite the stronger T cell reactivity observed during ruxolitinib discontinuation, no HIV-specific T cells could be identified during this period (Fig. 5e).

High frequency of $CD16^+CD56^-$ NK cells

NK cells have been proposed to play an important role in mediating the graft-versus-leukemia effect upon allo-HSCT, while their expansion and interaction with T cells may also regulate acute and chronic GvHD[28,29]. On the other hand, their implication in controlling HIV after ART interruption is suggested by recent reports[30–32]. Of note, IciS-34 underwent allo-HSCT with cells from a nine-of-ten HLA-matched donor. Among the matched alleles, there were three HLA class I alleles (A*24:02, B*27:05 and B*44:02) that intrinsically express the Bw4 ligand that is recognized by NK cells and whose presence has been associated with lower levels of HIV-1 viremia[33]. We therefore analyzed the phenotype and antiviral capacity of NK cells. While early after allo-HSCT, NK cells were characterized by a high proportion of immature $CD16^-CD56^{++}$ cells, a high proportion of experienced $CD16^+CD56^-$ cells expressing CD57 were observed at later timepoints (Fig. 6a,b). NK cells expressed different killer-cell immunoglobulin-like receptors (KIRs; Fig. 6c), such as KIR2DL1/S1, KIR2DL23 and, notably, KIR3DL1/S1, which are reported NK cell receptors for Bw4 (refs. 34–36). NK cell maturation, loss of CD56 and expression of CD57, was more preponderant among cells expressing KIRs and, in particular, KIR3DL1/S1 (Fig. 6b,c), suggesting a predominant activation of KIR-expressing cells in this case. The loss of CD56 expression has been proposed to identify NK cells with adaptive traits that became exhausted owing to repeated inflammatory and activating signals[37]. Although $CD16^+CD56^-$ NK cells are expanded during chronic HIV infection[38,39], the frequency observed here was higher than that in one person with HIV on ART whose cells were analyzed in parallel for reference (Fig. 6a and Supplementary Fig. 4b). The dynamics of NK cells in this case closely recapitulate the changes occurring in people without HIV who underwent allo-HSCT and experienced HCMV reactivation during the procedure[40]. Indeed, IciS-34 experienced three episodes of HCMV reactivation between August 2018 and March 2019 requiring valganciclovir treatment. HCMV reactivation was also detected between June 2019 and January 2020, but at levels that did not require treatment. We did not observe significant changes in the phenotype of NK cells during the brief period of ruxolitinib discontinuation (Fig. 6b and Supplementary Fig. 4c). While $CD16^+CD56^-$ NK cells have been reported to have poor cytotoxic and antiviral potential[38,39], we found that NK cells from IciS-34 were able to partially inhibit HIV-1 infection in vitro of autologous $CD4^+$ T cells (Fig. 6d). Further analyses will be needed to better understand the role that NK cells may have played in decreasing the HIV reservoir through graft-versus-HIV reservoir or direct antiviral effects.

Discussion

We describe the case of a person who underwent allo-HSCT with cells from a wild-type *CCR5* donor and whose viral load remains undetectable 32 months after interruption of ART. Multiple virological and immunological readouts confirm the absence of viral exposure since ART discontinuation and support a profound and prolonged HIV-1 remission in this individual.

At the time of allo-HSCT, this individual had been living with HIV for more than 30 years and had experienced several years of uncontrolled viremia, leading to a drop in $CD4^+$ T cell counts, before the virus was successfully controlled through an optimized protease inhibitor-based ART regimen. IPDA confirmed the presence of replication-competent virus in samples obtained during the period of suppressed viremia under ART before allo-HSCT. Cells carrying HIV DNA were readily detectable in blood and bone marrow samples just before the intervention, and residual viremia in the plasma was detected with an ultrasensitive technique at this time. A drastic drop in all these parameters was observed following allo-HSCT. However, previous cases of people with HIV who interrupted ART after wild-type *CCR5* allo-HSCT resulted in viral rebound within weeks to months of treatment discontinuation[11,41], confirming that the dramatic decline in the viral reservoirs associated with allo-HSCT is generally not sufficient to achieve HIV remission or cure.

The factors underlying the absence of viral rebound in the case presented here remain unclear. Sporadic (twice) pre-exposure prophylaxis use was reported by the participant and confirmed by pharmacological analyses, but given the long-term viral remission (now getting close to 3 years), we believe intermittent ART was not a major factor in the outcome of this case. Unknown host factors may hinder HIV reseeding and amplification from residual infected cells in this case. We found, however, that $CD4^+$ T cells obtained after ART interruption were fully susceptible to HIV-1 infection. Moreover, we could not identify any evidence of immune-driven control of infection. In particular, we could not find neutralizing antibodies or $CD8^+$ T cells able to suppress HIV infection. On the contrary, the lack of detectable HIV-specific T cells and the weak and waning antibody levels observed after ART interruption provide further evidence of the lack of viral reactivation events since allo-HSCT in this individual. Nevertheless, we cannot rule out a potential role of NK cells in mediating viral control. The combination of Bw4 ligands and KIRs present in this person after the transplant has been previously shown to favor natural viral control[35,36], and NK cells have the capacity to react to the expression of stress peptides on infected cells[42] before viral antigen production. Although the $CD16^+CD56^-$ NK population, highly abundant in this case, has been generally considered as functionally impaired[38,39], recent reports suggest that this population may be more heterogeneous than previously thought and that at least some of these cells possess diverse functionality, including cytotoxic potential[43,44]. A more thorough analysis of this compartment in this and other cases of people with HIV who required allo-HSCT will be needed to better understand the potential role of NK cells in controlling infection in this setting, either through graft-versus-reservoir effects or antiviral activities.

The immunosuppressive environment provided by ruxolitinib might contribute to the prevention of viral reactivation in this individual. This inhibitor of the JAK–STAT pathway was used to treat GvHD

https://doi.org/10.1038/s41591-024-03277-z

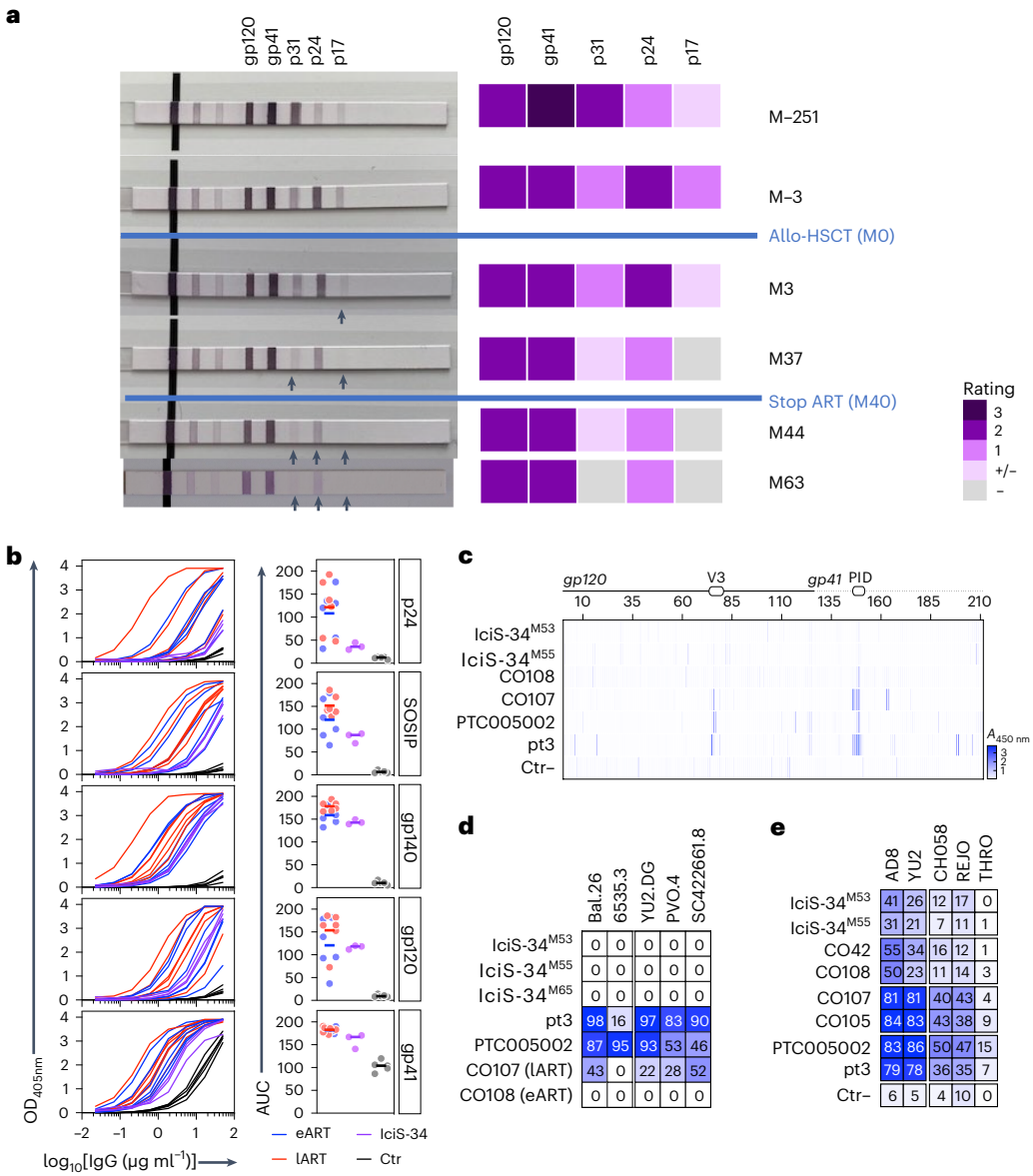

Fig. 4 | Antibody response after ART interruption. a, Results of immunoblots for HIV-1 antibodies in plasma samples from IciS-34 at different times before and after allo-HSCT. The arrows indicate the antigens against which reactivity was progressively lost. On the right are indicated the reactivity ratings that were automatically attributed for each antigen on the strips. **b**, ELISA graphs (left) comparing the reactivity of purified plasma IgG antibodies from IciS-34 (values for samples obtained at three different timepoints (M53, M55, M65) are depicted) and early- and late-treated PLWH (eART ($n = 6$) and lART ($n = 6$), respectively) against HIV-1 p24 and Env proteins. HIV-1-seronegative (Ctr−) sera ($n = 5$) were used as negative controls. Dot plots comparing the area under the curve (AUC) values calculated from the titration curves are shown on the right (horizontal lines indicate the median values). **c**, Heatmap showing the ELISA binding analysis of purified serum IgG antibodies from IciS-34 at two timepoints against consensus subtype B overlapping Env peptides. Darker colors indicate higher reactivity (absorbance values); white, no binding. Sera from eART (CO108), lART (CO107), post-treatment controller (PTC005002) and elite controller (pt3) individuals were used as positive controls. **d**, Heatmap comparing the in vitro neutralizing activity (as percentages) of purified serum IgG antibodies from IciS-34 (3 timepoints), CO108, CO107, PTC005002 and pt3 against selected clade B tier 1 and 2 viruses as measured in the TZM-bl assay. **e**, Heatmap comparing the percentage of CEM.NKR-CCR5 cells infected by laboratory-adapted (YU2 and AD8) and transmitted/founder viruses (CH058, REJO and THRO) bound by purified serum IgG antibodies from IciS-34 (2 timepoints), eART (CO42 and CO108), lART (CO105 and CO107), PTC005002 and pt3. HIV-1-seronegative (Ctr−) serum was used as negative control (**c**,**e**).

and has been administered almost continuously since ART interruption. Of note, ruxolitinib has been shown to block HIV replication, viral reactivation and reservoir reseeding in vitro and ex vivo and may favor the decay of the viral reservoir[45,46]. We found that the presence of ruxolitinib was indeed associated with a relative lack of reactivity of T cells from this individual to short stimulation in vitro. Ruxolitinib was briefly discontinued during the follow-up after ART interruption, and this was accompanied by an increase in T cell reactivity in vitro. The absence of ruxolitinib did not result in viral rebound or the appearance of HIV-specific cells, suggesting that no HIV antigens were produced during this period. It is possible, however, that the discontinuation of ruxolitinib (4 weeks) was too short for stochastic viral reactivation events to occur in a context in which potential remaining infected cells would be extremely rare.

Finally, we can hypothesize that allogenic immunity during repeated graft-versus-host events in this individual led to a deeper elimination of infected cells than in previous cases, achieving HIV cure through the complete purge of cells carrying replication-competent

https://doi.org/10.1038/s41591-024-03277-z

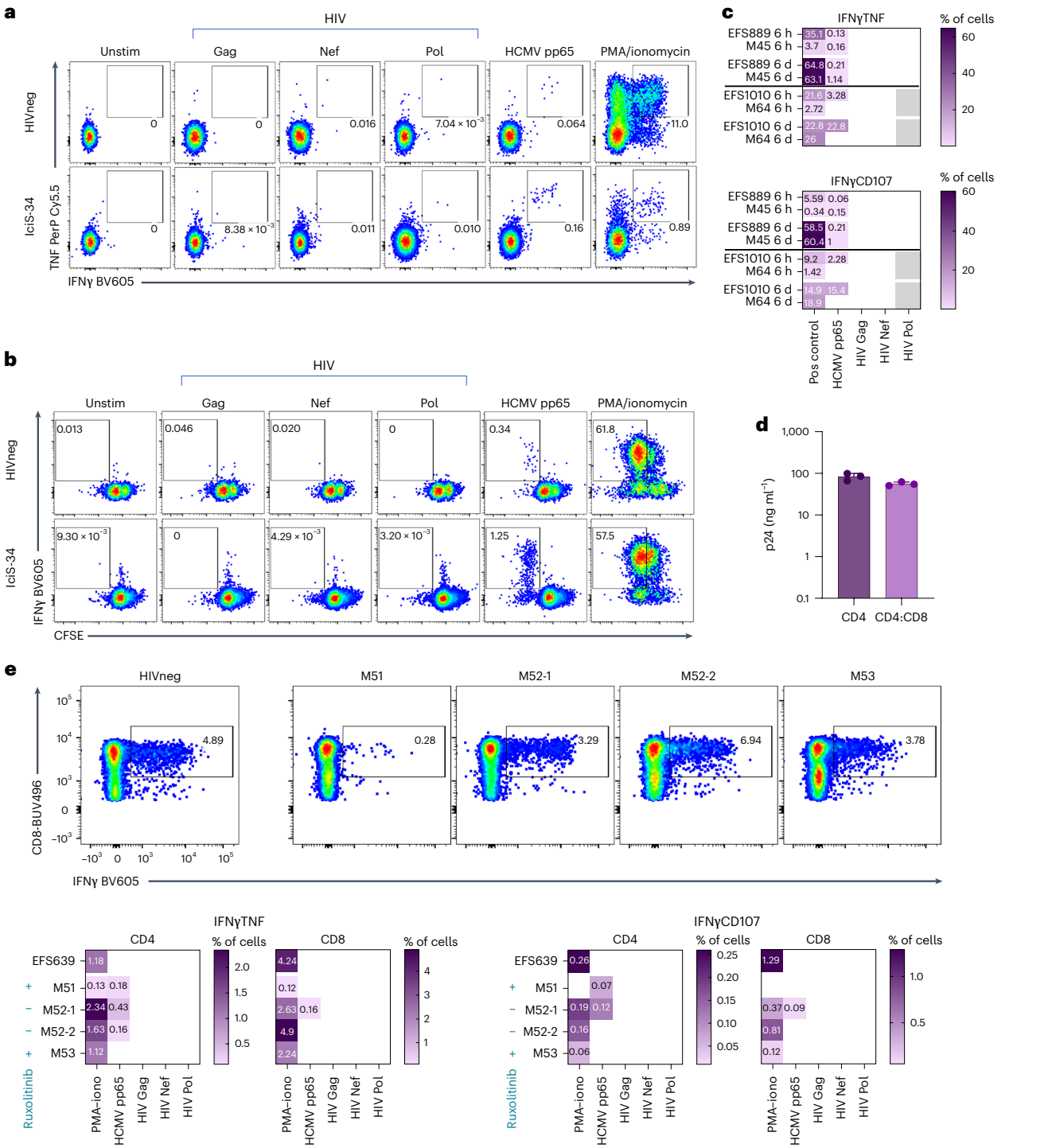

Fig. 5 | T cell reactivity and HIV-specific T cell response. a, Percentage of CD8$^+$ T cells from IciS-34 (M45) and an HIV-negative donor producing IFNγ and TNF after 6 h of stimulation with PMA/ionomycin, or with pools of HCMV pp65 peptides and HIV-1 Gag, Nef and Pol peptides. Unstimulated (Unstim) cells were used as control. Results are depicted as standard pseudocolor dot plots. **b**, Percentage of CD8$^+$ T cells from IciS-34 (M45) and an HIV-negative donor that proliferated (CFSE^{low}) after 6 days of stimulation with anti-CD3/CD28, pools of HCMV pp65 peptides, and HIV-1 Gag, Nef and Pol peptides and were able to produce IFNγ upon short polyclonal or antigen-specific restimulation. **c**, Heatmap comparing the percentage of CD8$^+$ T cells from IciS-34 (two samples) and two HIV-negative donors that produced IFNγ and/or TNF and IFNγ and/or expressed CD107 after 6 h or 6 days (**d**) of polyclonal (positive control, Pos) or antigen-specific stimulation. Darker colors indicate higher percentages. White, undetectable; gray, not done. The percentages are indicated after subtraction of the background from the unstimulated condition. **d**, Comparison of the level of infection of CD4$^+$ T cells from IciS-34 (M45) infected in vitro with HIV-1_{BaL} cultured alone or in the presence of autologous CD8$^+$ T cells (1:1 ratio). The results are shown as the levels of p24 in culture supernatants at day 7 after infection in vitro (mean ± s.d. of 3 experiments). Similar results were obtained at M54, M56, M57 and M59. **e**, Percentage of CD8$^+$ T cells from an HIV-negative donor and IciS-34 at time of ruxolitinib discontinuation (M51), 15 days after ruxolitinib discontinuation (M52-1), 4 weeks after ruxolitinib discontinuation, time of reinitiation (M52-2) and 15 days after ruxolitinib reinitiation (M53), producing IFNγ 6 h after polyclonal stimulation with PMA/ionomycin (top). Heatmap comparing the percentages of CD4$^+$ and CD8$^+$ T cells from the HIV-negative donor and IciS-34 at different timepoints that produced IFNγ and/or TNF and IFNγ and/or expressed CD107 after 6 h of polyclonal or antigen-specific stimulation.

https://doi.org/10.1038/s41591-024-03277-z

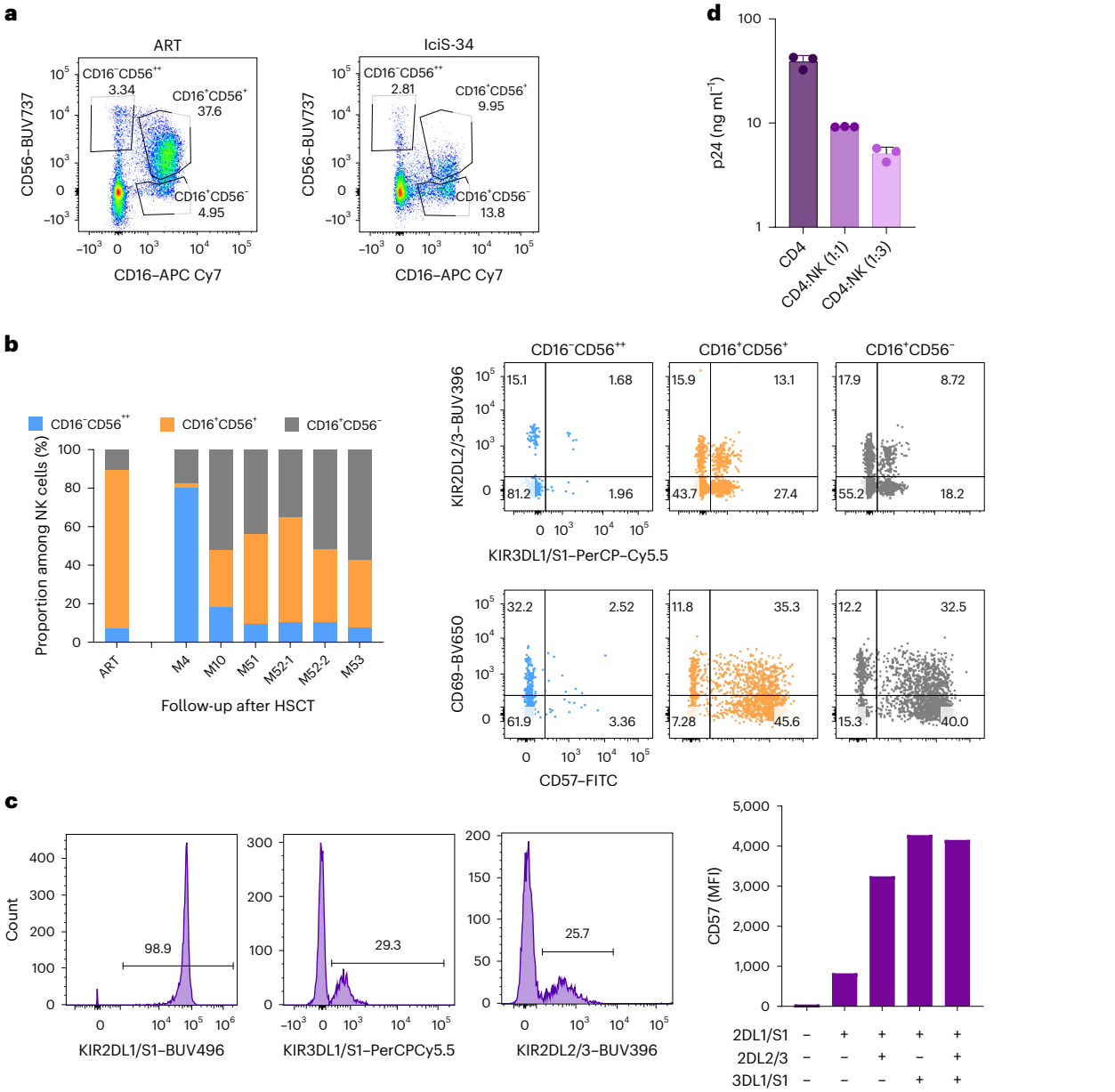

Fig. 6 | Phenotype and antiviral activity of NK cells. a, Expression of CD16 and CD56 on NK cells from one person with HIV on ART and IciS-34 (M52-2). **b**, Proportion of $CD16^{-}CD56^{++}$, $CD16^{+}CD56^{+}$ and $CD16^{+}CD56^{-}$ NK cells in the sample from the person on ART and from IciS-34 at six different timepoints (left). Expression of KIR2DL2/3 and/or KIR3DL1/S1 and CD69 and/or CD57 in the three NK cell subsets from IciS-34 (M52-2) (right). **c**, Expression of CD57 on NK cell subsets from IciS-34 (M52-2) defined on the absence or expression of different combinations of KIRs. MFI, median fluorescence intensity. **d**, Comparison of the level of infection of $CD4^{+}$ T cells from IciS-34 (M59) infected in vitro with HIV-1_{BaL} cultured alone or in the presence of autologous NK cells (1:1 and 1:3 ratios). The results are shown as the levels of p24 in culture supernatants at day 3 after infection in vitro (mean ± s.d. of three experiments). Similar results were obtained at M54.

viruses. In favor of an allogenic pressure on the HIV reservoir in this case is the progressive rarefaction after the transplant of cells carrying viral DNA, which were detected at trace levels in several samples in the months that followed the transplant. The need for graft-versus-host reactions to achieve HIV cure after allo-HSCT has been the subject of debate: while its impact on the HIV reservoir is increasingly clear (graft-versus-reservoir effects)[15,47], the incidence of GvH in the reported cases of HIV cure after allo-HSCT was variable[5–9]. Of note, a recent study in a model of allo-HSCT in Simian immunodeficiency virus (SIV)-infected macaques has shown that allogeneic immunity can in some cases lead to the total clearance of the viral reservoir[16]. Recently, a mathematical model was applied to data from IciStem participants, including data from IciS-34 before ART interruption[15]. The model supports the hypothesis that the main driver of the strong reservoir reduction after allo-HSCT is graft-versus-reservoir effects rather than conditioning regimens. It is tempting to assume that the repeated graft-versus-host reactions in this case may have led to an efficient elimination of reservoir cells in the absence of the barrier provided by *CCR5Δ32*.

Allo-HSCT is not a therapeutic option for people with HIV who do not have a cancer requiring this approach. Nevertheless, allo-HSCT is the only medical intervention that has reproducibly led to profound remission and potential cure of HIV-1 infection. The case presented here is the first to achieve such outcome after receiving cells from a

wild-type *CCR5* donor. It is unclear whether the status that this person has achieved will be permanent. We cannot exclude that he may harbor rare, infected cells with competent provirus or that viral rebound may occur if immunosuppressive drugs are discontinued for longer periods of time. Viral rebound can occur even after long periods of undetectable viremia without ART, as observed in the so-called Mississippi baby[48]. Because of the absence of an intrinsic resistance to infection, the risk of viral rebound may be considered higher than for the cases of allo-HSCT with *CCR5Δ32* cells. However, the duration of undetectable viremia is unprecedented in this context. This case opens new perspectives for the development of HIV cure strategies, particularly concerning allogeneic immunity and immunosuppressive drugs.

Online content

Any methods, additional references, Nature Portfolio reporting summaries, source data, extended data, supplementary information, acknowledgements, peer review information; details of author contributions and competing interests; and statements of data and code availability are available at https://doi.org/10.1038/s41591-024-03277-z.

References

1. Namazi, G. et al. The Control of HIV After Antiretroviral Medication Pause (CHAMP) study: posttreatment controllers identified from 14 clinical studies. *J. Infect. Dis.* **218**, 1954–1963 (2018).
2. Sáez-Cirión, A. et al. Post-treatment HIV-1 controllers with a long-term virological remission after the interruption of early initiated antiretroviral therapy ANRS VISCONTI study. *PLoS Pathog.* **9**, e1003211 (2013).
3. Li, J. Z. et al. Time to viral rebound after interruption of modern antiretroviral therapies. *Clin. Infect. Dis.* **74**, 865–870 (2022).
4. Passaes, C. et al. Early antiretroviral therapy favors post-treatment SIV control associated with the expansion of enhanced memory $CD8^+$ T-cells. *Nat. Commun.* **15**, 178 (2024).
5. Gupta, R. K. et al. HIV-1 remission following CCR5Δ32/Δ32 haematopoietic stem-cell transplantation. *Nature* **568**, 244–248 (2019).
6. Hsu, J. et al. HIV-1 remission and possible cure in a woman after haplo-cord blood transplant. *Cell* **186**, 1115–1126.e1118 (2023).
7. Hutter, G. et al. Long-term control of HIV by CCR5 Delta32/Delta32 stem-cell transplantation. *N. Engl. J. Med.* **360**, 692–698 (2009).
8. Jensen, B.-E. O. et al. In-depth virological and immunological characterization of HIV-1 cure after CCR5Δ32/Δ32 allogeneic hematopoietic stem cell transplantation. *Nat. Med.* **29**, 583–587 (2023).
9. Dickter, J. K. et al. HIV-1 remission after allogeneic hematopoietic-cell transplantation. *N. Engl. J. Med.* **390**, 669–671 (2024).
10. Liu, R. et al. Homozygous defect in HIV-1 coreceptor accounts for resistance of some multiply-exposed individuals to HIV-1 infection. *Cell* **86**, 367–377 (1996).
11. Henrich, T. J. et al. Antiretroviral-free HIV-1 remission and viral rebound after allogeneic stem cell transplantation: report of 2 cases. *Ann. Intern. Med* **161**, 319–327 (2014).
12. Salgado, M. et al. Mechanisms that contribute to a profound reduction of the HIV-1 reservoir after allogeneic stem cell transplant. *Ann. Intern. Med.* **169**, 674–683 (2018).
13. Cummins, N. W. et al. Extensive virologic and immunologic characterization in an HIV-infected individual following allogeneic stem cell transplant and analytic cessation of antiretroviral therapy: a case study. *PLoS Med.* **14**, e1002461 (2017).
14. Koelsch, K. K. et al. Impact of allogeneic hematopoietic stem cell transplantation on the HIV reservoir and immune response in 3 HIV-infected individuals. *J. Acquir. Immune Defic. Syndr.* **75**, 328–337 (2017).
15. Salgado, M. et al. Dynamics of virological and immunological markers of HIV persistence after allogeneic haematopoietic stem-cell transplantation in the IciStem cohort: a prospective observational cohort study. *Lancet HIV* **11**, e389–e405 (2024).
16. Wu, H. L. et al. Allogeneic immunity clears latent virus following allogeneic stem cell transplantation in SIV-infected ART-suppressed macaques. *Immunity* **56**, 1649–1663.e5 (2023).
17. Ambinder, R. F. et al. Allogeneic hematopoietic cell transplant for HIV patients with hematologic malignancies: the BMT CTN-0903/AMC-080 Trial. *Biol. Blood Marrow Transplant.* **25**, 2160–2166 (2019).
18. Huyveneers, L. E. P. et al. Autopsy study defines composition and dynamics of the HIV-1 reservoir after allogeneic hematopoietic stem cell transplantation with CCR5Delta32/Delta32 donor cells. *Viruses* **14**, 2069 (2022).
19. Eberhard, J. M. et al. Vulnerability to reservoir reseeding due to high immune activation after allogeneic hematopoietic stem cell transplantation in individuals with HIV-1. *Sci. Transl. Med.* **12**, eaay9355 (2020).
20. Kordelas, L. et al. Shift of HIV tropism in stem-cell transplantation with *CCR5* Delta32 mutation. *N. Engl. J. Med.* **371**, 880–882 (2014).
21. Murray, D. D. et al. Altered immune reconstitution in allogeneic stem cell transplant recipients with human immunodeficiency virus (HIV). *Clin. Infect. Dis.* **72**, 1141–1146 (2021).
22. Avettand-Fenoel, V. et al. Dynamics in HIV-DNA levels over time in HIV controllers. *J. Int. AIDS Soc.* **22**, e25221 (2019).
23. Bruner, K. M. et al. A quantitative approach for measuring the reservoir of latent HIV-1 proviruses. *Nature* **566**, 120–125 (2019).
24. Passaes, C. P. B. et al. Ultrasensitive HIV-1 p24 assay detects single infected cells and differences in reservoir induction by latency reversal agents. *J. Virol.* **91**, e02296-16 (2017).
25. Fonsart, J. et al. Single-dose pharmacokinetics and pharmacodynamics of oral tenofovir and emtricitabine in blood, saliva and rectal tissue: a sub-study of the ANRS IPERGAY trial. *J. Antimicrob. Chemother.* **72**, 478–485 (2017).
26. International, H. I. V. C. S. et al. The major genetic determinants of HIV-1 control affect HLA class I peptide presentation. *Science* **330**, 1551–1557 (2010).
27. Parampalli Yajnanarayana, S. et al. JAK1/2 inhibition impairs T cell function in vitro and in patients with myeloproliferative neoplasms. *Br. J. Haematol.* **169**, 824–833 (2015).
28. Hadjis, A. D. & McCurdy, S. R. The role and novel use of natural killer cells in graft-versus-leukemia reactions after allogeneic transplantation. *Front. Immunol.* **15**, 1358668 (2024).
29. Simonetta, F., Alvarez, M. & Negrin, R. S. Natural killer cells in graft-versus-host-disease after allogeneic hematopoietic cell transplantation. *Front. Immunol.* **8**, 465 (2017).
30. Climent, N. et al. Immunological and virological findings in a patient with exceptional post-treatment control: a case report. *Lancet HIV* **10**, e42–e51 (2023).
31. Etemad, B. et al. HIV post-treatment controllers have distinct immunological and virological features. *Proc. Natl Acad. Sci. USA* **120**, e2218960120 (2023).
32. Essat, A. et al. A genetic fingerprint associated with durable HIV remission after interruption of antiretroviral treatment. Anrs Visconti. Preprint at *SSRN* https://doi.org/10.2139/ssrn.4540849 (2023).
33. Flores-Villanueva, P. O. et al. Control of HIV-1 viremia and protection from AIDS are associated with HLA-Bw4 homozygosity. *Proc. Natl Acad. Sci. USA* **98**, 5140–5145 (2001).
34. Alter, G. et al. Differential natural killer cell-mediated inhibition of HIV-1 replication based on distinct KIR/HLA subtypes. *J. Exp. Med.* **204**, 3027–3036 (2007).
35. Martin, M. P. et al. Epistatic interaction between *KIR3DS1* and *HLA-B* delays the progression to AIDS. *Nat. Genet.* **31**, 429–434 (2002).

36. Martin, M. P. et al. Innate partnership of HLA-B and KIR3DL1 subtypes against HIV-1. *Nat. Genet.* **39**, 733–740 (2007).
37. Lugli, E., Marcenaro, E. & Mavilio, D. NK cell subset redistribution during the course of viral infections. *Front. Immunol.* **5**, 390 (2014).
38. Hu, P. F. et al. Natural killer cell immunodeficiency in HIV disease is manifest by profoundly decreased numbers of $CD16^{+}CD56^{+}$ cells and expansion of a population of $CD16^{dim}CD56^{-}$ cells with low lytic activity. *J. Acquir. Immune Defic. Syndr. Hum. Retrovirol.* **10**, 331–340 (1995).
39. Mavilio, D. et al. Characterization of $CD56^{-}/CD16^{+}$ natural killer (NK) cells: a highly dysfunctional NK subset expanded in HIV-infected viremic individuals. *Proc. Natl Acad. Sci. USA* **102**, 2886–2891 (2005).
40. Zaghi, E. et al. Single-cell profiling identifies impaired adaptive NK cells expanded after HCMV reactivation in haploidentical HSCT. *JCI Insight* **6**, e146973 (2021).
41. Avettand-Fenoel, V. et al. Failure of bone marrow transplantation to eradicate HIV reservoir despite efficient HAART. *AIDS* **21**, 776–777 (2007).
42. Long, E. O. & Rajagopalan, S. Stress signals activate natural killer cells. *J. Exp. Med.* **196**, 1399–1402 (2002).
43. Forconi, C. S. et al. A new hope for $CD56^{neg}CD16^{pos}$ NK cells as unconventional cytotoxic mediators: an adaptation to chronic diseases. *Front. Cell. Infect. Microbiol.* **10**, 162 (2020).
44. Orrantia, A. et al. A NKp80-based identification strategy reveals that $CD56^{neg}$ NK cells are not completely dysfunctional in health and disease. *iScience* **23**, 101298 (2020).
45. Gavegnano, C. et al. Novel mechanisms to inhibit HIV reservoir seeding using Jak inhibitors. *PLoS Pathog.* **13**, e1006740 (2017).
46. Gavegnano, C. et al. Ruxolitinib and tofacitinib are potent and selective inhibitors of HIV-1 replication and virus reactivation in vitro. *Antimicrob. Agents Chemother.* **58**, 1977–1986 (2014).
47. Prator, C. A., Donatelli, J. & Henrich, T. J. From Berlin to London: HIV-1 reservoir reduction following stem cell transplantation. *Curr. HIV/AIDS Rep.* **17**, 385–393 (2020).
48. Luzuriaga, K. et al. Viremic relapse after HIV-1 remission in a perinatally infected child. *N. Engl. J. Med.* **372**, 786–788 (2015).

Asier Sáez-Cirión[1,2] ✉, Anne-Claire Mamez[3], Véronique Avettand-Fenoel[4,5,6], Mitja Nabergoj[7], Caroline Passaes[1,2], Paul Thoueille[8,9], Laurent Decosterd[8], Maxime Hentzien[10], Federico Perdomo-Celis[2], Maria Salgado[11,12,13], Monique Nijhuis[14,15], Adeline Mélard[4], Elise Gardiennet[4], Valérie Lorin[16], Valérie Monceaux[1,2], Anaïs Chapel[1,2], Maël Gourvès[1], Marine Lechartier[1], Hugo Mouquet[16], Annemarie Wensing[17,18], Javier Martinez-Picado[11,12,13,19,20], Sabine Yerly[21], Mathieu Rougemont[22] & Alexandra Calmy[10] ✉

[1]Viral Reservoirs and Immune Control Unit, Université Paris Cité, Institut Pasteur, Paris, France. [2]HIV Inflammation and Persistence Unit, Université Paris Cité, Institut Pasteur, Paris, France. [3]Division of Hematology, Department of Oncology, Geneva University Hospitals, Geneva, Switzerland. [4]Institut Cochin—CNRS 8104/INSERM U1016/Université de Paris, Paris, France. [5]LI2RSO, Université d'Orléans, Orléans, France. [6]Virologie, CHU d'Orléans, Orléans, France. [7]Institut Central des Hôpitaux, Sion, Switzerland. [8]Service of Clinical Pharmacology, Department of Laboratory Medicine and Pathology, Lausanne University Hospital and University of Lausanne, Lausanne, Switzerland. [9]Service of Clinical Pharmacology, Department of Medicine, Lausanne University Hospital and University of Lausanne, Lausanne, Switzerland. [10]HIV/AIDS Unit, Division of Infectious Diseases, Geneva University Hospitals, Geneva, Switzerland. [11]IrsiCaixa, Badalona, Spain. [12]Germans Trias i Pujol Research Institute, Badalona, Spain. [13]CIBERINFEC, Instituto de Salud Carlos III, Madrid, Spain. [14]Translational Virology Research Group, Department of Medical Microbiology, University Medical Center Utrecht, Utrecht, The Netherlands. [15]HIV Pathogenesis Research Unit, Faculty of Health Sciences, University of the Witwatersrand, Johannesburg, South Africa. [16]Humoral Immunology Unit, Inserm U1222, Université Paris Cité, Institut Pasteur, Paris, France. [17]Translational Virology Research Group, Department of Global Public Health & Bioethics, Julius Center for Health Sciences and Primary Care, University Medical Center Utrecht, Utrecht, The Netherlands. [18]Ezintsha, Faculty of Health Sciences, University of the Witwatersrand, Johannesburg, South Africa. [19]UVic-UCC, Vic, Spain. [20]ICREA, Barcelona, Spain. [21]Laboratory of Virology, Geneva University Hospitals, Geneva, Switzerland. [22]Unaffiliated, Geneva, Switzerland. ✉e-mail: asier.saez-cirion@pasteur.fr; alexandra.calmy@hug.ch

Methods

Ethics

The described individual was enrolled in 1992 in the Swiss HIV Cohort Study (SHCS; www.shcs.ch) and in 2018 as participant number 34 in the IciStem (IciS-34) program (www.icistem.org) at the Hôpitaux Universitaires de Genève after giving signed consent. The SHCS was approved by the Cantonal Ethics Commission at Zürich (the Central Ethics Commission in Switzerland for the SHCS), and the IciStem study by the ethical committee at the Universitair Medisch Centrum Utrecht. HSCT was done in the context of the standard protocol at Hôpitaux Universitaires de Genève. The individual signed a consent form for the use of samples for research purposes according to the regulations of the Hôpitaux Universitaires de Genève.

The decision to stop ART was reached consensually between the participant and his attending physicians after a period of treatment simplification, which was implemented to diminish the risk of interactions with immunosuppressors used to treat GvHD. Analyses from unrelated HIV-negative blood donors from the Etablissement Français du Sang (collaboration agreement with Institut Pasteur) and people with HIV on ART (with undetectable viremia for >24 months) from the ANRS EP36 XII mTOR study (approved by ethics committee Ile-de-France XI) are provided as reference.

Sample processing

Peripheral blood was collected in EDTA tubes. Fresh blood samples were centrifuged at 750*g* for 20 min to collect the plasma. A second centrifugation was made at 2,000*g* for 30 min to eliminate platelets. Plasma samples were stored at −80 °C. PBMCs were obtained by density gradient centrifugation following Ficoll Plaque Plus separation (GE Healthcare) and used fresh or cryopreserved in liquid nitrogen.

Ultrasensitive plasma viremia

Ultrasensitive HIV RNA quantifications were performed on large volumes of plasma using the Generic (Biocentric) or Abbott HIV real-time PCR assay (Abbott)[12,22]. In brief, 3.5–17.5 ml of plasma was ultra-concentrated at 170,000*g* at 4 °C for 30 min, after which viral RNA was extracted. HIV RNA was quantified with a validated in-house calibration curve, set with a limit of detection of 0.56 copies per milliliter.

Cell-associated HIV DNA and RNA levels

Total DNA was isolated from frozen PBMCs or CD4$^+$ T cells sorted from PBMCs (StemCell Technologies) using the DNeasy Kit (Qiagen). Total HIV DNA was quantified with an ultrasensitive method using the real-time PCR GENERIC HIV-DNA assay (Biocentric)[22,49]

Cell-associated RNA was extracted from PBMCs with an AllPrep DNA/RNA Mini Kit (Qiagen). During extraction, cell-associated HIV RNA was treated using DNase I (Qiagen). Cell-associated HIV RNA was quantified by semi-nested real-time PCR targeting the gag region with previously described primers and probes[50] shown in Supplementary Table 5. Reverse transcription was performed with random hexamers and SuperScript IV (Invitrogen). The first PCR was performed with Taq ADN polymerase (Merck) for 15 cycles, then the product of the first PCR was used as a template in the second PCR. The semi-nested real-time PCR was performed with Platinum qPCR SuperMix-UDG w/ROX (Invitrogen) for 50 cycles. To normalize cell-associated HIV RNA per µg total RNA, ribosomal RNA was quantified from the same cDNA by real-time PCR using the Ribosomal RNA Control Reagents kit (Applied Biosystems).

IPDA

The presence of potentially intact DNA HIV-1 was determined in PBMCs using a duplex droplet digital PCR (QX200 ddPCR system, Bio-Rad) targeting two regions in the viral genome[23]: the packaging signal in the 5′ and the Rev response element in env in the 3′. Genomic DNA was extracted using the AllPrep DNA/RNA Mini Kit (Qiagen) with precautions to minimize DNA shearing. To normalize and calculate DNA shearing, a second duplex droplet digital PCR was used, targeting the human *RPP30* gene. Primers and probes were previously described and are shown in Supplementary Table 6.

CD4$^+$ T cell culture for viral amplification

CD4$^+$ T cells were isolated from fresh PBMCs after positive selection with magnetic beads (EasySep Human CD4 Positive Selection Kit II, StemCell Technologies, 17852). Cells were stimulated with phytohemagglutinin-L (2 µg ml^{-1}, Sigma-Aldrich, L4144) and IL-2 (200 UI ml^{-1}, Miltenyi Biotec, 130-097-746). After 3 days of stimulation, cells from IciS-34 (1×10^6–2×10^6 cells) were put in culture with a pre-activated pool of HIV-susceptible CD4$^+$ T cells from 3 HIV-negative donors (1:3 ratio of total cells) at a final concentration of 10^6 ml^{-1} in RPMI 1640 with glutamax (Gibco, 61870-044) supplemented with 10% heat-inactivated fetal calf serum and IL-2 at 200 UI ml^{-1}. Culture supernatants were collected every 3 to 4 days and fresh medium was added to the cultures. Supernatants were stored at −80 °C before analysis.

HIV-1 p24 was analyzed by ultrasensitive digital ELISA (Simoa Quanterix). Cell supernatants were thawed at room temperature and centrifuged at 845*g* for 5 min; 200 µl was transferred into a SimOa 96-well plate and inactivated with 20 µl of Triton 20%. HIV-1 Gag p24 was determined on a Simoa HD-1 analyzer using the Simoa HIV p24 kit (Quanterix, 102215) following the manufacturer's instructions. Four-parameter logistic regression fitting was used to estimate the concentration of p24. Samples below the limit of quantification were based on the established cutoff (it was determined based on the p24 average number of enzymes per bead (AEB) signal in the standard 0 and calculated as 2.5 standard deviations from the mean of the p24 AEB signal).

CD4$^+$ T cell susceptibility to HIV-1 infection

Productive HIV-1 infection in vitro was studied in activated CD4$^+$ T cells (10^6 cells per ml in triplicate) exposed to the HIV-1_{BaL} strain (R5; p24 10 ng ml^{-1}). The cells were cultured in 96-U-well plates for 14 days. Every 3–4 days, the culture supernatants were removed and replaced with fresh culture medium. Viral replication was monitored in the supernatants by p24 ELISA (XpressBio). Single-round infections were performed with HIV-1 NL4.3ΔenvΔnef/GFP (ref. 51) pseudotyped with the VSV-G envelope protein by transiently cotransfecting (SuperFect; Qiagen) 293 T cells with the proviral vectors and the VSV-G expression vector pMD2.G. Activated CD4$^+$ T cells were infected in triplicate (5×10^4 cells per well, 200 µl) with 35 ng per 1×10^6 HIV-1 NL4.3Δnef/GFP/VSV-G. Active HIV-1 infection was estimated by flow cytometry (BD Fortessa, BD Biosciences) as the percentage of GFP-expressing CD4$^+$ T cells 72 h after infection.

Flow cytometry phenotyping

T cell phenotyping. Frozen PBMCs were thawed and incubated overnight in RPMI, 10% fetal bovine serum, 1% penicillin–streptomycin and IL-15 (0.1 ng ml^{-1}, Miltenyi Biotec). Cells were stained with a Live/Dead Fixable Aqua Dead Cell Stain Kit (Life Technologies) followed by surface staining (CD3–FITC (SK7, 344804, dilution 1:13, BioLegend), CD4–BUV496 (OKT4, 750977, 1:65, BD Biosciences), CD8–BUV496 (RPA-T8, 612942, 1:65, BD Biosciences), CCR5–PECy7 (2D7, 557752, 1:7, BD Biosciences), CXCR4–PE (12G5, 555974, 1:7, BD Biosciences), CD45RA–APC_H7 (HI100, 560674, 1:26, BD Biosciences), CCR7–PE_Dazzle_594 (G043H7, 353236, 1:13, BioLegend), CD27–APC_R700 (M-T271, 565116, 1:26, BD Biosciences), HLA-DR–BV786 (G46-6, 564041, 1:26, BD Biosciences), CD38–BV605 (HIT2, 740401, 1:65, BD Biosciences) and Brilliant Stain Buffer Plus (563794, 1:3, BD Biosciences)). For intranuclear staining, cells were fixed and permeabilized (Cytofix/Cytoperm, BD Biosciences) and stained with anti-Ki67-eFluor450 (20Raj1, 48-5699-42, 1:26, eBioscience). All samples were acquired on an LSRFortessa

flow cytometer (BD Biosciences). The differentiation into naive, central memory, transitional memory, effector memory and late effector T cells over time was analyzed via the expression of CCR7, CD27 and CD45RA (Supplementary Fig. 3a).

NK cell phenotyping. Frozen PBMCs were thawed and incubated overnight in RPMI, 10% fetal bovine serum, 1% penicillin–streptomycin and IL-15 (0.1 ng ml^{-1}, Miltenyi Biotec). Cells were stained with a Live/Dead Fixable Aqua Dead Cell Stain Kit (L34957, 1:2,000, Life Technologies) followed by surface staining (KIR2DL2/L3–BUV395 (clone CH-L, 743456, 1:40), KIR2DL1/S1–BUV496 (clone HP-MA4, 752510, 1:40), CD25–BUV661 (clone M-A251, 741608, 1:40), CD56–BUV737 (clone NCAM16.2, 612766, 1:20), CD14–V450 (clone M5E2, 558121, 1:250), CD19–V450 (clone HIB19, 560353, 1:20), NKG2A–BV605 (clone 131411, 747921, 1:80), CD69–BV650 (clone FN50, number 563835, 1:20), DNAM1–BV711 (clone DX11, 564796, 1:20), NKG2C–BV786 (clone 134591, 748170, 1:25), CD57–FITC (clone NK-1, 555619, 1:5), NKp46–PECy7 (clone 9E2, 562101, 1:20), CD3–AF700 (clone UCHT1, 557943, 1:50), CD16–APC Cy7 (clone 3G8, 560195, 1:20) (all from BD Biosciences); CD85j/LILRB1–PE (clone REA998, 130-116-615, 1:50), NKG2D–PE Vio615 (clone REA1228, 130-124-352, 1:50), KIR3DL1/S1–PerCPVio700 (clone REA168, 130-124-077, 1:50), NKp30–APC (clone REA823, 130-112-431, 1:50) (from Miltenyi)). The gating schemes applied to identify NK cells are shown in Supplementary Fig. 4. Boolean gating was performed with FlowJo (v10.9) and the following markers: KIR3DL1/S1, KIR2DL1/S1 and KIRDL2/3. Data were acquired using an LSRFortessa X20 flow cytometer (BD Biosciences).

T cell stimulation

Cryopreserved PBMCs were thawed in RPMI 1640 Medium, GlutaMAX Supplement, complemented with 20% fetal bovine serum. Cells were split and partly stained with carboxyfluorescein succinimidyl ester (CFSE) at 1 µM (Invitrogen, C34554) for 6 days of stimulation experiments. All cells were then kept overnight at 37 °C and 5% CO_2.

6 h of stimulation. PBMCs were resuspended in RPMI 1640 Medium, GlutaMAX with 10% fetal bovine serum in the presence of anti-CD107a–BUV396 (clone H4A3, 565113,1:200) and BD FastImmune Co-stimulatory Antibodies CD28/CD49d (1 µg ml^{-1}; BD, 347690) and left unstimulated or stimulated with either hCMV pp65 peptide pool (2 µg ml^{-1}), HIV Gag peptides (2 µg ml^{-1}), HIV Nef peptides (2 µg ml^{-1}) (all of them obtained through the NIH HIV reagents program) or soluble anti-CD3 (clone OKT3, 1 µg ml^{-1}, eBioscience, 16-0037-85) and anti-CD28 (clone CD28.2, 1 µg ml^{-1}, eBioscience, 16-0289-85). After 30 min of incubation, brefeldin A (10 µg ml^{-1}; Invitrogen, 00-4506-51) and BD GolgiStop Protein Transport Inhibitor (containing monensin) (1 µg ml^{-1}, BD, 554724) were added and cells were cultured for 5 h 30 min before flow cytometry staining.

6 days of stimulation. CFSE-labeled PBMCs were resuspended in RPMI 1640 Medium, GlutaMAX Supplement, complemented with 10% fetal bovine serum and left unstimulated or stimulated in the same conditions as described above. Following 6 days of culture, cells were resuspended with anti-CD107a_BUV395 (clone H4A3, BD Biosciences, 565113, 1:200), brefeldin A and BD GolgiStop Protein Transport Inhibitor (containing monensin) and were left unstimulated or restimulated overnight with hCMV pp65 peptide pool (2 µg ml^{-1}), HIV Gag peptides (2 µg ml^{-1}), HIV Nef peptides (2 µg ml^{-1}), or phorbol 12-myristate 13-acetate (PMA) (80 ng ml^{-1}, Sigma-Aldrich, P8139-5MG) and ionomycin (500 ng ml^{-1}, Sigma-Aldrich, I0634-5MG).

In all conditions, samples were stained using the Live/Dead Fixable Aqua Dead Cell Stain Kit (Invitrogen; L34957), then extracellular staining was performed using CD3–APCe780 (clone UCHT1, 47-0038-42, 1:9, Biolegend), CD4–BUV737 (clone OKT4, 750977, 1:36, BD Biosciences), CD8–BUV496 (clone RPA-T8, 612942, 1:36, BD Biosciences), CCR7–PEDazzle594 (clone G043H7, 353236, 1:7, Biolegend), CD45RA PECy7 (clone 5H9, 561216, 1:14, BD Biosciences) and CD27 APCR700 (clone M-T271, 565116, 1:14, BD Biosciences) antibodies. The cells were fixed and permeabilized with the BD Cytofix/Cytoperm Fixation/Permeabilization Kit (BD Biosciences) and stained for IFNγ BV605 (clone B27, 560679, 1:6, BD Biosciences), and TNF PerCP Cy5.5 (clone Mab11, 560679, 1:6, BD Biosciences) before analysis with an LSRFortessa X20 flow cytometer (BD Biosciences).

Viral suppression assays

HIV-1 suppression was evaluated with fresh blood samples[52]. After PBMC isolation from peripheral blood, CD4$^+$ T cells were separated by positive magnetic bead isolation (EasySep Human CD4 Positive Selection Kit II, 17852) and the remaining cell fraction was split for subsequent CD8$^+$ T cell and NK cell negative selection (EasySep Human CD8$^+$ Cell Enrichment Kit, 19053; EasySep Human NK Enrichment Kit, 19055) using a Robosep instrument (StemCell Technology). Purified cells were cultured in RPMI 1640 medium containing GlutaMAX, 10% fetal bovine serum, penicillin (10 UI ml^{-1}) and streptomycin (10 µg ml^{-1}). After purification, CD4$^+$ T cells were activated for 3 days with 2 µg ml^{-1} of phytohemagglutinin-L (Sigma, L4144) and 200 IU ml^{-1} of IL-2 (human IL-2 IS, premium grade, Miltenyi Biotec, 130-097-745). In parallel, CD8$^+$ T cells and NK cells were cultured in complete RPMI medium in the absence of cytokines (CD8$^+$ T cells) or in the presence of IL-15 at 0.1 ng ml^{-1} (NK cells). Activated CD4$^+$ T cells were infected with HIV-1_{BaL} by spinoculation alone or with autologous CD8$^+$ T cells (1:1 ratio) or NK cells (1:1 and 1:3 ratio). Cells were then cultured for 14 days in interleukin-2 (100 IU ml^{-1})-supplemented complete RPMI. Supernatants were collected and fresh medium replenished every 3–4 days. Viral replication was measured in terms of p24 production in the culture supernatants by means of ELISA (HIV-1 p24 ELISA kit, XpressBio, XB-1000). The viral inhibitory capacity of NK cells was calculated comparing p24 levels at day 3 after infection in the NK:CD4 co-cultures to CD4$^+$ T cells cultured alone. The viral inhibitory capacity of CD8$^+$ T cells was calculated at day 7 after infection as the log drop in p24 production when CD4$^+$ T cells were cultured in the presence of CD8$^+$ T cells.

Analysis of anti-HIV antibodies

Initial screening for HIV antibodies in plasma samples was done using INNO-LIA HIV Score immunoblot (Fujirebio). For deeper characterization, IgG antibodies were purified from plasma samples by affinity chromatography using Protein G Sepharose 4 Fast Flow (Cytvia, 17061805) according to the manufacturer's instructions. Purified plasma antibodies were dialyzed against PBS using Slide-A-Lyzer Cassettes (10 K molecular weight cutoff, Thermo Fisher Scientific). Final IgG concentrations were measured using a NanoDro One instrument (Thermo Fisher Scientific). Previously purified plasma IgG antibodies from early treated (eART), late treated (lART), elite controller (Pt3), and post-treatment controller (PTC005002) donors[53–55] were used as controls in the following experiments.

Titration of antibody levels by ELISAs. High-binding 96-well ELISA plates (Costar, Corning) were coated overnight with purified Env proteins (His-tagged clade B YU2 trimeric gp140 and monomeric gp120 (ref. 56), BG505 SOSIP.664 (ref. 57), gp41 (group O HIV-1 and 2, 227-20101, RayBiotech) and HxB2 p24 (produced from the expression plasmid number ARP-13137, NIH AIDS reagent program; 125 ng per well in PBS). After washing with 0.05% Tween 20-PBS (PBST), plates were blocked for 2 h with 2% bovine serum albumin and 1 mM EDTA–PBST (blocking solution), washed and incubated with 1:3 serially diluted purified IgG antibodies in PBS (maximum concentration of 50 µg ml^{-1}). After washing, plates were revealed by the addition of goat-HRP-conjugated anti-human IgG (1:2,000, 109-035-098, Jackson ImmunoResearch) and HRP chromogenic substrate (ABTS solution; Euromedex)[58,59].

Overlapping linear HIV-1 Env peptides (n = 211, consensus Subtype B Env peptide set, 9480, BEI Resources) were coated on high-binding 96-well ELISA plates (Costar, Corning) at 10 µg ml^{-1} in PBS overnight. After washing with 0.1% Tween 20–PBS, plates were blocked for 2 h with 1% Tween 20, 5% sucrose and 3% milk–PBS (blocking solution); washed with 0.1% Tween 20–PBS; and incubated with purified IgG antibodies at 10 µg ml^{-1} in 1% BSA and 0.1% Tween 20–PBS. Plates were revealed by the addition of secondary antibody and substrate as described. Experiments were performed using a HydroSpeed microplate washer and Sunrise microplate absorbance reader (Tecan), with absorbance measured at 450 nm ($A_{450\,nm}$). All antibodies were tested in duplicate in at least two independent experiments.

HIV-1 neutralization assay. Pseudoviruses (BaL.26 (11446), 6535.3 (11017), YU2.DG (12133), SC422661.8 (11058) and PVO.4 (11022); Env plasmids obtained from the NIH AIDS reagent program) were prepared by co-transfection of HEK-293T cells (CRL-3216, ATCC) with pSG3Δenv vector (11051, NIH AIDS Reagent Program) using FUGENE-6 transfection reagent (Promega)[60,61]. Neutralization experiments were performed by incubating in triplicate IgG antibodies at a final concentration of 250 µg ml^{-1} with pseudoviruses for 1 h at 37 °C. The virus–IgG mixtures were then used to infect 10,000 TZM-bl cells (8129, NIH AIDS Reagent Program) in the presence of 10 µg ml^{-1} of diethylaminoethyl (DEAE)–dextran. Infection levels were determined after 48 h by measuring the luciferase activity of cell lysates.

Antibody binding to infected cells. The capacity of purified antibodies to bind to HIV-1-infected cells was evaluated using laboratory-adapted (AD8 (11346) and YU2 (1350)) and transmitted/founder (CH058 (11856), REJO (11746) and THRO (11745)) viruses produced from infectious molecular clones (NIH HIV Reagent Program). CEM.NKR-CCR5 cells (4376, NIH HIV Reagent Program) were infected with inocula of selected viruses and adjusted to achieve 10–40% of Gag$^+$ cells at 48 h after infection. Infected cells were incubated with purified IgG antibodies (50 µg ml^{-1} final concentration) in staining buffer (0.5% BSA, 2 mM EDTA–PBS) for 30 min at 37 °C, washed and incubated with AF647-conjugated anti-human IgG antibodies (1:400; A-21445, Life Technologies) for 30 min at 4 °C. Cells were then fixed with 4% paraformaldehyde and stained for intracellular Gag using FITC-conjugated anti-HIV-1 core FITC KC57 (1:500, 6604665, Beckman Coulter)[62]. Data were acquired using an Attune Nxt instrument (Life Technologies) and analyzed using FlowJo software (v10.7.1; FlowJo LLC).

Screening of antiretrovirals

The screening of antiretrovirals in plasma samples was performed using three distinct multiplex liquid chromatography coupled to tandem mass spectrometry (LC–MS/MS) methods. Bictegravir, cabotegravir, cobicistat, darunavir, dolutegravir, doravirine, elvitegravir, raltegravir, rilpivirine and ritonavir (pool A) were analyzed using a Vanquish system hyphenated to a TSQ Quantiva triple quadrupole MS. The chromatographic column was a Waters Xselect HSS T3 3.5 µm, 2.1 × 75 mm, kept at 35 °C in the LC oven. The mobile phase was made of water and acetonitrile (ACN) with 0.1% formic acid in each. The gradient program ranged from 10% to 95% ACN plus formic acid in 3.6 min, and the total method duration (including equilibration for the next injection) was 5.5 min. The flow rate and injection volume were 0.5 ml min^{-1} and 5 µl, respectively. For the analysis of atazanavir, efavirenz, etravirine, lopinavir, maraviroc, nevirapine and saquinavir (pool B), the gradient program ranged from 2% to 95% ACN plus formic acid in 2.81 min and the total method duration (including equilibration for the next injection) was 4.5 min. The analysis of abacavir, emtricitabine, lamivudine, tenofovir and zidovudine (pool C) was performed using a Vanquish system hyphenated to a TSQ Altis triple quadrupole MS. The chromatographic column was a Waters Xselect HSS T3 3.5 µm, 2.1 × 75 mm, kept at room temperature. The gradient program ranged from 0 to 70% ACN in 3 min, and the total method duration (including equilibration for the next injection) was 5 min. The flow rate and injection volume were 0.4 ml min^{-1} and 3 µl, respectively.

For the sample preparation, 150 µl of the precipitation solution containing the isotopically labeled internal standards was added to an aliquot of 50 µl of plasma for protein precipitation. For pools A and B, the mixture was then centrifugated for 10 min at 14,000g (5 °C) and the supernatant was directly injected. For pool C, the mixture was centrifugated for 10 min at 12,700g (5 °C) and the supernatant was diluted 1:1 with fresh Milli-Q water before injection.

Statistics and reproducibility

Graphs were generated using Prism version 10 (GraphPad Software). Flow cytometry data were analyzed using FlowJo cytometry analysis software v10.7 or v10.9 (Tree Star).

As this study was focused on one specific male individual, several limitations need to be noted: influence of sex or gender could not be considered; no statistical method was used to predetermine sample size; the experiments were not randomized; the investigators were not blinded to allocation during experiments and outcome assessment.

Samples at different timepoints (biological replicates) were measured in all experiments except HIV DNA determinations in gut biopsies. Technical triplicates were measured for viral suppression assays, neutralization assays and CD4$^+$ T cell susceptibility to HIV-1 infection, and duplicates for antibody titers. All replication attempts produced consistent results. No data were excluded from the analyses.

Reporting summary

Further information on research design is available in the Nature Portfolio Reporting Summary linked to this article.

Data availability

The data that support the findings of this study are presented in the main figures and Supplementary Information of this Article. Supporting data will be available within 6 weeks upon request to the corresponding authors, except when there are constraints related to the protection of the participant's privacy.

References

49. Bosman, K. J. et al. Development of sensitive ddPCR assays to reliably quantify the proviral DNA reservoir in all common circulating HIV subtypes and recombinant forms. *J. Int. AIDS Soc.* **21**, e25185 (2018).
50. Pasternak, A. O. et al. Highly sensitive methods based on seminested real-time reverse transcription-PCR for quantitation of human immunodeficiency virus type 1 unspliced and multiply spliced RNA and proviral DNA. *J. Clin. Microbiol.* **46**, 2206–2211 (2008).
51. Amara, A. et al. G protein-dependent CCR5 signaling is not required for efficient infection of primary T lymphocytes and macrophages by R5 human immunodeficiency virus type 1 isolates. *J. Virol.* **77**, 2550–2558 (2003).
52. Saez-Cirion, A., Shin, S. Y., Versmisse, P., Barre-Sinoussi, F. & Pancino, G. Ex vivo T cell-based HIV suppression assay to evaluate HIV-specific CD8$^+$ T-cell responses. *Nat. Protoc.* **5**, 1033–1041 (2010).
53. Molinos-Albert, L. M. et al. Transient viral exposure drives functionally-coordinated humoral immune responses in HIV-1 post-treatment controllers. *Nat. Commun.* **13**, 1944 (2022).
54. Planchais, C. et al. HIV-1 treatment timing shapes the human intestinal memory B-cell repertoire to commensal bacteria. *Nat. Commun.* **14**, 6326 (2023).
55. Scheid, J. F. et al. Sequence and structural convergence of broad and potent HIV antibodies that mimic CD4 binding. *Science* **333**, 1633–1637 (2011).

56. Scheid, J. F. et al. Broad diversity of neutralizing antibodies isolated from memory B cells in HIV-infected individuals. *Nature* **458**, 636–640 (2009).
57. Sok, D. et al. Recombinant HIV envelope trimer selects for quaternary-dependent antibodies targeting the trimer apex. *Proc. Natl Acad. Sci. USA* **111**, 17624–17629 (2014).
58. Mouquet, H. et al. Memory B cell antibodies to HIV-1 gp140 cloned from individuals infected with clade A and B viruses. *PLoS ONE* **6**, e24078 (2011).
59. Mouquet, H. et al. Complex-type N-glycan recognition by potent broadly neutralizing HIV antibodies. *Proc. Natl Acad. Sci. USA* **109**, E3268–E3277 (2012).
60. Li, M. et al. Human immunodeficiency virus type 1 env clones from acute and early subtype B infections for standardized assessments of vaccine-elicited neutralizing antibodies. *J. Virol.* **79**, 10108–10125 (2005).
61. Sarzotti-Kelsoe, M. et al. Optimization and validation of the TZM-bl assay for standardized assessments of neutralizing antibodies against HIV-1. *J. Immunol. Methods* **409**, 131–146 (2014).
62. Bruel, T. et al. Elimination of HIV-1-infected cells by broadly neutralizing antibodies. *Nat. Commun.* **7**, 10844 (2016).

Acknowledgements

We warmly thank Romuald, also known as the Geneva patient, described here, for his generosity and commitment. We also thank the Swiss HIV Cohort Study (www.SHCS.ch) supported by the Swiss National Science Foundation (grant number 201369), SHCS project number P889 and the IciStem study for their helpful contribution. The IciStem program (www.icistem.org) was funded through the AmfAR Research Consortium on HIV Eradication (ARCHE) program (AmfAR 109858-64-RSRL) and the Dutch Aidsfonds (P60802). A list of all members can be found in Supplementary Information. F.P.-C. was supported by Institut Pasteur's Roux Cantarini program. A. Chapel was supported by a grant from ANRS Emerging Infectious Diseases (ANRS-MIE). M.G. was supported by UM1AI164562, co-funded by the National Heart Lung and Blood Institute (NHLBI), National Institute of Diabetes and Digestive and Kidney Diseases (NIDDK), National Institute of Neurological Disorders and Stroke (NINDS), National Institute on Drug Abuse (NIDA), and the National Institute of Allergy and Infectious Diseases (NIAID). J.M.P. is supported by the Spanish Ministry of Science, Innovation and Universities (grants PID2022-139271OB-I00 and CB21/13/ 00063) and NIH/NIAID (1P01AI178376-01). The funders had no role in the study design, data collection and analysis, decision to publish or preparation of the paper.

Author contributions

A.S.-C. and A. Calmy coordinated this work. A.S.-C., A.-C.M., V.A.-F., M. Nabergoj, M.S., M. Nijhuis, A.W., J.M.P., S.Y., M.R. and A. Calmy conceived and designed the study. A.S.-C., V.A.-F., C.P., P.T., L.D., M.H., F.P.-C., M.S., M. Nijhuis, A.M., E.G., V.L., V.M., A. Chapel, M.G., M.L., H.M., A.W., J.M.P. and S.Y. designed and/or performed the experiments. A.S.-C., V.A.-F., C.P., P.T., L.D., M.S., M. Nijhuis, H.M., A.W., J.M.P., S.Y. and A. Calmy performed the analyses and/or interpreted the data. A.-C.M., M. Nabergoj, M.H., S.Y., M.R. and A. Calmy were involved in the clinical management of the patient and/or collected and handled patient samples. A.S.-C., A.-C.M., V.A.-F., H.M. and A. Calmy wrote the draft of the paper. All authors critically reviewed the paper and contributed important intellectual content.

Competing interests

The authors declare no competing interests.

Additional information

Supplementary information The online version contains supplementary material available at https://doi.org/10.1038/s41591-024-03277-z.

Correspondence and requests for materials should be addressed to Asier Sáez-Cirión or Alexandra Calmy.

Peer review information *Nature Medicine* thanks Timothy Henrich and the other, anonymous, reviewer(s) for their contribution to the peer review of this work. Primary Handling Editors: Alison Farrell and Liam Messin, in collaboration with the *Nature Medicine* team.

nature portfolio

Corresponding author(s): Asier SAEZ-CIRION

Last updated by author(s): Aug 19, 2024

Reporting Summary

Nature Portfolio wishes to improve the reproducibility of the work that we publish. This form provides structure for consistency and transparency in reporting. For further information on Nature Portfolio policies, see our Editorial Policies and the Editorial Policy Checklist.

Statistics

For all statistical analyses, confirm that the following items are present in the figure legend, table legend, main text, or Methods section.

n/a	Confirmed
☐	☒ The exact sample size (*n*) for each experimental group/condition, given as a discrete number and unit of measurement
☒	☐ A statement on whether measurements were taken from distinct samples or whether the same sample was measured repeatedly
☒	☐ The statistical test(s) used AND whether they are one- or two-sided *Only common tests should be described solely by name; describe more complex techniques in the Methods section.*
☒	☐ A description of all covariates tested
☒	☐ A description of any assumptions or corrections, such as tests of normality and adjustment for multiple comparisons
☐	☒ A full description of the statistical parameters including central tendency (e.g. means) or other basic estimates (e.g. regression coefficient) AND variation (e.g. standard deviation) or associated estimates of uncertainty (e.g. confidence intervals)
☒	☐ For null hypothesis testing, the test statistic (e.g. *F*, *t*, *r*) with confidence intervals, effect sizes, degrees of freedom and *P* value noted *Give P values as exact values whenever suitable.*
☒	☐ For Bayesian analysis, information on the choice of priors and Markov chain Monte Carlo settings
☒	☐ For hierarchical and complex designs, identification of the appropriate level for tests and full reporting of outcomes
☒	☐ Estimates of effect sizes (e.g. Cohen's *d*, Pearson's *r*), indicating how they were calculated

Our web collection on statistics for biologists contains articles on many of the points above.

Software and code

Policy information about availability of computer code

Data collection	Flow cytometry data acquisition was conducted using an LSR Fortessa (BD Biosciences)
Data analysis	Graphs were generated using Prism version 10 (GraphPad Software). Flow cytometry data analysis and Boolean gating were performed with FlowJo (v10.7 and v10.9)

For manuscripts utilizing custom algorithms or software that are central to the research but not yet described in published literature, software must be made available to editors and reviewers. We strongly encourage code deposition in a community repository (e.g. GitHub). See the Nature Portfolio guidelines for submitting code & software for further information.

Data

Policy information about availability of data

All manuscripts must include a data availability statement. This statement should provide the following information, where applicable:

- Accession codes, unique identifiers, or web links for publicly available datasets
- A description of any restrictions on data availability
- For clinical datasets or third party data, please ensure that the statement adheres to our policy

The data that support the findings of this study are presented in the main figures and supplemental material of this article. Source data will be available within six weeks upon request to the corresponding authors, except data protection constraints related to the protection of the participant's privacy.

Research involving human participants, their data, or biological material

Policy information about studies with human participants or human data. See also policy information about sex, gender (identity/presentation), and sexual orientation and race, ethnicity and racism.

Reporting on sex and gender	Sex could not be considered in this study since it is focused on the characterization of one single case (male).
Reporting on race, ethnicity, or other socially relevant groupings	These parameters were not considered for this case report
Population characteristics	This study includes the description of a male participant, who was 53 years old at the time of this report. HLA genotype and detailed relevant diagnosis and therapeutic history are provided
Recruitment	The described individual was enrolled in the Swiss HIV cohort study (www.shcs.ch) and as participant #34 in the IciStem (IciS-34) program (www.icistem.org) at the Hôpitaux Universitaires de Genève after signed consent.
Ethics oversight	The described individual was enrolled in 1992 in the Swiss HIV cohort study (www.shcs.ch) and in 2018 as participant #34 in the IciStem (IciS-34) program (www.icistem.org) at the Hôpitaux Universitaires de Genève after signed consent. The Swiss HIV cohort study was approved by the Cantonal Ethics Commission at Zürich and the IciStem study by the ethical committee at the Universitair Medisch Centrum Utrecht. HSCT was done in the context of the standard protocol at Hôpitaux Universitaires de Genève. The individual signed a consent form for the use of samples for research purposes according to the regulations of the Hôpitaux Universitaires de Genève. Analyses from unrelated HIV negative blood donors from the Etablissement Français du Sang (collaboration agreement with Institut Pasteur) and people with HIV on ART (with undetectable viremia for >24 months) from the ANRS EP36 XII mTOR study (approved by ethics committee Ile-de-France XI) are provided as reference

Note that full information on the approval of the study protocol must also be provided in the manuscript.

Field-specific reporting

Please select the one below that is the best fit for your research. If you are not sure, read the appropriate sections before making your selection.

☒ Life sciences ☐ Behavioural & social sciences ☐ Ecological, evolutionary & environmental sciences

For a reference copy of the document with all sections, see nature.com/documents/nr-reporting-summary-flat.pdf

Life sciences study design

All studies must disclose on these points even when the disclosure is negative.

Sample size	Sample size calculation was not applicable as this study was focused on one specific individual
Data exclusions	No data exclusion
Replication	Samples at different time points (biological replicates) were measured in all experiments except HIV-DNA determinations in gut biopsies. Technical triplicates were measured for viral suppression assays, neutralization assays and CD4+ T cells susceptibility to HIV-1 infection, and duplicates for antibody titers. All replication attempts produced consistent results.
Randomization	Not Applicable since the study was focused on a single case
Blinding	Not Applicable since the study was focused on a single case

Reporting for specific materials, systems and methods

We require information from authors about some types of materials, experimental systems and methods used in many studies. Here, indicate whether each material, system or method listed is relevant to your study. If you are not sure if a list item applies to your research, read the appropriate section before selecting a response.

Materials & experimental systems

n/a	Involved in the study
☐	☒ Antibodies
☐	☒ Eukaryotic cell lines
☒	☐ Palaeontology and archaeology
☒	☐ Animals and other organisms
☒	☐ Clinical data
☒	☐ Dual use research of concern
☒	☐ Plants

Methods

n/a	Involved in the study
☒	☐ ChIP-seq
☐	☒ Flow cytometry
☒	☐ MRI-based neuroimaging

Antibodies

Antibodies used

T cell stimulation
CD3 (clone OKT3, 1µg/mL, eBioscience, ref #16-0037-85) and CD28 (clone CD28.2, 1µg/mL, eBioscience, ref #16-0289-85)

T cell phenotyping
CD3-FITC (SK7, #344804, dilution 1/13, BioLegend), CD4-BUV496 (OKT4, #750977, 1/65, BD Bioscience), CD8-BUV496 (RPA-T8, #612942, 1/65, BD Bioscience), CCR5-PECy7 (2D7, #557752, 1/7, BD biosciences), CXCR4-PE (12G5, #555974, 1/7, BD Bioscience), CD45RA-APC_H7 (HI100, #560674, 1/26, BD Bioscience), CCR7-PE_Dazzle_594 (G043H7, #353236, 1/13, BioLegend), CD27-APC_R700 (M-T271, #565116, 1/26, BD), HLA-DR-BV786 (G46-6, #564041, 1/26, BD Bioscience), CD38-BV605 (HIT2, #740401, 1/65, BD Bioscience), Brilliant Stain buffer plus (#563794, 1/3, BD Bioscience). anti-Ki67-eFluor450 (20Raj1, #48-5699-42, 1/26, eBioscience

NK cell phenotping
(KIR2DL2/L3-BUV395 (clone CH-L), #743456, dilution 1/40), KIR2DL1/S1- BUV496 (clone HP-MA4), , #752510, 1/40), CD25-BUV661 (clone M-A251, #741608, 1/40), CD56-BUV737 (clone NCAM16.2, #612766, 1/20), CD14-V450 (clone M5E2, #558121, 1/250), CD19-V450 (clone HIB19, #560353, 1/20), NKG2A-BV605 (clone 131411, #747921, 1/80), CD69-BV650 (clone FN50, #563835, 1/20), DNAM1-BV711 (clone DX11, #564796, 1/20), NKG2C-BV786 (clone 134591, #748170, 1/25), CD57-FITC (clone NK-1, #555619, 1/5), NKp46-PE Cy7 (clone 9E2, #562101, 1/20), CD3-AF700 (clone UCHT1, #557943, 1/50), CD16-APC Cy7 (clone 3G8, #560195, 1/20) (all from BD Biosciences); CD85j/LILRB1-PE (clone REA998, #130-116-615, 1/50), NKG2D-PE Vio615 (clone REA1228, #130-124-352, 1/50), KIR3DL1/S1-PerCPVio700 (clone REA168, #130-124-077, 1/50), NKp30-APC (clone REA823, #130-112-431, 1/50) (from Miltenyi).

ICS
CD3-APCe780 (clone UCHT1, #47-0038-42, dilution 1/9, Biolegend), CD4-BUV737 (clone OKT4, #750977, 1/36, BD Bioscience), CD8-BUV496 (clone RPA-T8, #612942, 1/36, BD Bioscience), CCR7-PEDazzle594 (clone G043H7, #353236, 1/7, Biolegend), CD45RA PECy7 (clone 5H9, #561216, 1/14, BD Bioscience), CD27 APCR700 (clone M-T271, #565116, 1/14, BD Bioscience), for IFNγ BV605 (clone B27, #560679, 1/6, BD Bioscience), and TNFα PerCP Cy5.5 (clone Mab11, #560679, 1/6, BD Bioscience), anti-CD107a_BUV395 (clone H4A3, BD Bioscience, #565113, 1/200)

Analysis of anti-HIV antibodie
HRP-conjugated anti-human IgG (1:2000 dilution, #109-035-098, Jackson ImmunoResearch)
AF647-conjugated anti-human IgG antibodies (1:400 dilution; #A-21445, Life Technologies)
FITC-conjugated anti-HIV-1 core FITC KC57 (1:500 dilution, #6604665, Beckman Coulter)

Validation

Manufacturer's Specifications: We reviewed the manufacturer's specifications and technical data sheets for each antibody. This information included details such as clone names, isotypes, recommended dilutions, and references.
Positive and Negative Controls: To validate antibody performance, we used positive and negative controls. Positive controls included cells known to express the target antigen, while negative controls were cells lacking the antigen.
Fluorescence Minus One (FMO) Controls: FMO controls were utilized to assess background fluorescence.

Eukaryotic cell lines

Policy information about cell lines and Sex and Gender in Research

Cell line source(s)

HEK-293T cells (CRL-11268™, ATCC).
TZM-bl cells (#8129, NIH AIDS Reagent Program).
CEM.NKR-CCR5+ cells (#4376, NIH AIDS Reagent Program).

Authentication

Authentication was based on morphology, growth and expected behaviour and functionality.

Mycoplasma contamination

Mycoplasma contamination not tested.

Commonly misidentified lines
(See ICLAC register)

Misidentified lines were not used.

Plants

Seed stocks	N/A
Novel plant genotypes	N/A
Authentication	N/A

Flow Cytometry

Plots

Confirm that:

☒ The axis labels state the marker and fluorochrome used (e.g. CD4-FITC).

☒ The axis scales are clearly visible. Include numbers along axes only for bottom left plot of group (a 'group' is an analysis of identical markers).

☒ All plots are contour plots with outliers or pseudocolor plots.

☒ A numerical value for number of cells or percentage (with statistics) is provided.

Methodology

Sample preparation	Immunophenotyping of lymphocyte populations was performed on cryopreserved Peripheral Blood Mononuclear Cells Cells (PBMC). Cryopreserved PBMCs were thawed in RPMI 1640 Medium, GlutaMAX Supplement, complemented with 20% FCS.
Instrument	Fortessa flow cytometer (BD Biosciences).
Software	FlowJo software version v10.9 (Tree Star Inc.).
Cell population abundance	CD4+ T cells, CD8+ T cells and NK cells used for functional assays were sorted with magnetic beads. All fractions used had a purity above 90% based on flow cytometry analysis of populations as defined below.
Gating strategy	Lymphocytes were gated based on FSC-A/SSC-A, followed by single cell selection based on SSC-A/SSC-H. Live cells were then gated upon negative selection of cells labeled with LIVE/DEAD fixable Aqua Dead cekk Stain Kit. T cell subpopulations were defined based on expression of CD3, CD4, CD8, CD45RA, CCR7, CD27. NK cells were defined based on expression of CD16, CD56 among CD3neg, CD14neg, CD19neg cells See supplementary material for full gating strategy

☒ Tick this box to confirm that a figure exemplifying the gating strategy is provided in the Supplementary Information.